

REVIEW ARTICLE

Three-dimensional printing as a cutting-edge, versatile and personalizable vascular stent manufacturing procedure: Toward tailor-made medical devices

Fatima Garcia-Villen^{1,2,3*}, Fernando López-Zárraga⁴, Cesar Viseras^{5,6}, Sandra Ruiz-Alonso^{1,2,3}, Fouad Al-Hakim^{1,2,3}, Irene Diez-Aldama¹, Laura Saenz-del-Burgo^{1,2,3}, Denis Scaini^{7*}, Jose Luis Pedraz^{1,2,3}

¹NanoBioCel Group, School of Pharmacy, University of the Basque Country (UPV/EHU), 01006, Vitoria-Gasteiz, Spain

²Biomedical Research Networking Center in Bioengineering, Biomaterials and Nanomedicine (CIBER-BBN), 01006, Vitoria-Gasteiz, Spain

³Bioaraba, NanoBioCel Research Group, 01009, Vitoria-Gasteiz, Spain

⁴Department of Vascular and Interventional Radiology, Álava University Hospital, Integrated Health Organization of Álava (Osakidetza), Spain

⁵Department of Pharmacy and Pharmaceutical Technology, School of Pharmacy, University of Granada (UGR), Campus of Cartuja, 18071 s/n, Granada, Spain

⁶Andalusian Institute of Earth Sciences, CSIC-University of Granada, Avda. de Las Palmeras 4, 18100, Armilla, Granada, Spain

⁷Joint Research Laboratory (JRL). School of Pharmacy, University of the Basque Country (UPV/EHU), 01006, Vitoria-Gasteiz, Spain

***Corresponding authors:**

Fatima Garcia-Villen
(fatima.garciav@ehu.es)
Denis Scaini
(deniscaini@ehu.es)

Citation: Garcia-Villen F, López-Zárraga F, Viseras C, *et al.*, 2023, Three-dimensional printing as a cutting-edge, versatile and personalizable vascular stent manufacturing procedure: Toward tailor-made medical devices. *Int J Bioprint*, 9(2): 664.
<https://doi.org/10.18063/ijb.v9i2.664>

Received: August 09, 2022

Accepted: October 11, 2022

Published Online: January 9, 2023

Copyright: © 2023 Author(s). This is an Open Access article distributed under the terms of the Creative Commons Attribution License, permitting distribution and reproduction in any medium, provided the original work is properly cited.

Publisher's Note: Whioce Publishing remains neutral with regard to jurisdictional claims in published maps and institutional affiliations.

(This article belongs to the *Special Issue: 3D Tissue Engineering and Bioprinting for Emerging Applications*)

Abstract

Vascular stents (VS) have revolutionized the treatment of cardiovascular diseases, as evidenced by the fact that the implantation of VS in coronary artery disease (CAD) patients has become a routine, easily approachable surgical intervention for the treatment of stenosed blood vessels. Despite the evolution of VS throughout the years, more efficient approaches are still required to address the medical and scientific challenges, especially when it comes to peripheral artery disease (PAD). In this regard, three-dimensional (3D) printing is envisaged as a promising alternative to upgrade VS by optimizing the shape, dimensions and stent backbone (crucial for optimal mechanical properties), making them customizable for each patient and each stenosed lesion. Moreover, the combination of 3D printing with other methods could also upgrade the final device. This review focuses on the most recent studies using 3D printing techniques to produce VS, both by itself and in combination with other techniques. The final aim is to provide an overview of the possibilities and limitations of 3D printing in the manufacturing of VS. Furthermore, the current situation of CAD and PAD pathologies is also addressed, thus highlighting the main weaknesses of the already existing VS and identifying research gaps, possible market niches and future directions.

Keywords: Stent; Three-dimensional printing; Endovascular prosthesis; Atherosclerosis; Peripheral artery disease; Coronary artery disease

1. Introduction

Atherosclerosis and thrombosis are vascular conditions that represent one of the major causes of death worldwide^[1-3], thus placing a substantial medical and economic burden to society. The progressive and chronic accumulation of fat in artery walls, which is initially asymptomatic, can ultimately lead to the production of atheroma that blocks the vessel lumen, thus jeopardizing blood circulation. Moreover, atheroma plaques can also suffer from ruptures, causing local problems such as thrombosis, arterial wall ulcers, and dissection. If atherosclerosis happens in coronary arteries (coronary artery disease [CAD]), the blockage of the blood flow could lead to myocardial infarction and ultimately, death. If stenosis is located in other blood vessels of the peripheral circulatory system, it is known as peripheral artery disease (PAD). Even if PAD can affect any blood vessel, it is more common in the lower extremities than in the arms. It is also worth to clarify that PAD and CAD could have different causes, but atherosclerosis remains one of the most common causes.

Different medical approaches can be performed depending on the risk, age, stage of the condition, type of lesion, etc. Normally, when the artery blockage is severe, cardiologists resort to endovascular procedures or open vascular reconstruction. Regarding endovascular procedures, balloon angioplasty or endovascular stent are the most extended methods for treating the complications of atherosclerosis.

Up to 42% of CAD patients have PAD, and half of those patients are asymptomatic^[4]. According to Bauersachs *et al.*, “worldwide data showed approximately

5%–8% prevalence of CAD and 10%–20% prevalence of PAD, dependent on the study design, average age, gender, and geographical location”^[5]. Another recent report from the American Heart Association states that the lifetime risk of PAD has been estimated between 19% and 30% depending on the race, from white to black people, respectively^[6]. Chronic ulceration is one of the major problems of PAD, which could ultimately lead to amputation. Ulceration in these patients is related to disturbed microcirculation, swelling and edema^[7]. Due to the silent nature of atherosclerosis, it is very common for patients to suffer from cardiovascular events, thus needing hospitalization, surgery, and pharmacological treatments. Both CAD and PAD have demonstrated to be a significant economic burden on different health systems (Figure 1A). In particular, PAD represents a higher economic expense than CAD, especially due to a worse prognosis. In patients with PAD, cardiac complications are the major cause of morbidity and mortality. Moreover, the peripheral lesions are more complex and vaster than coronary ones^[8].

According to a recent market study made by IMARC Group Company, they expect the vascular stent (VS) market to steadily grow in the coming years. They ascribe this growth to the increasing trend of geriatric population as well as to a rise in the incidence rate of PAD, aortic aneurysm and ischemic heart disease^[9]. Nevertheless, if we look into the global VS market by product type, it is also clear that the majority of the efforts are centered on coronary stents (Figure 1B), relegating peripheral stents to a secondary place, despite being the condition with the most economic expenditure. In view of the above,

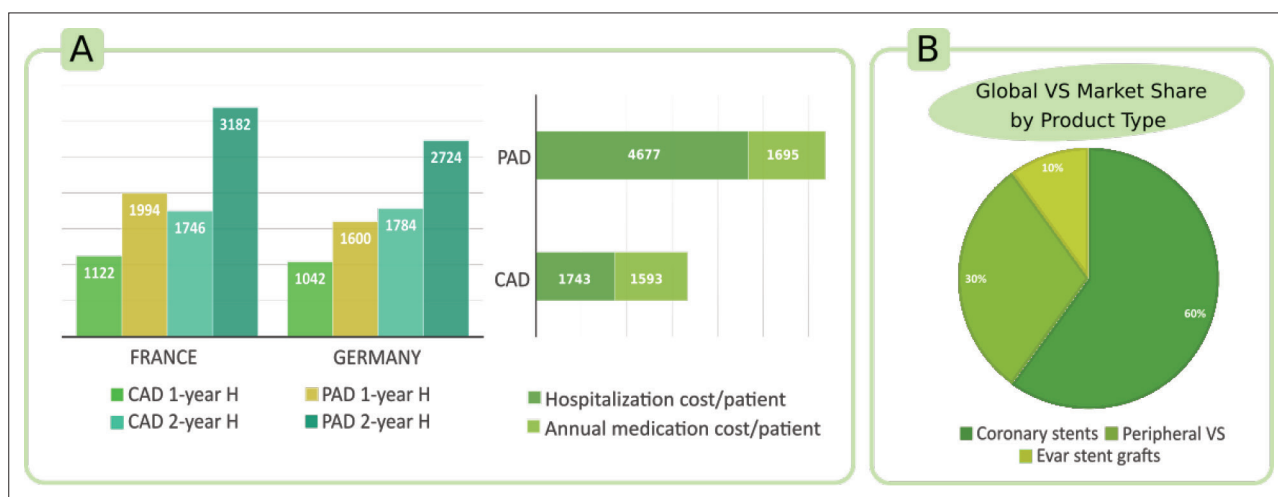


Figure 1. (A) Economic burden caused by CAD and PAD in France, Germany, and Canada. Left: average cumulative 1-year and 2-year direct medical costs associated with hospitalization/patient for both CAD and PAD (H stands for “hospitalization”). Extracted from Smolderen *et al.*^[145] Right: Average hospitalization and annual medication costs per patient in Canada. Extracted from Bauersachs *et al.*^[5]. Bars numbers correspond to amount in euros. (B) Global vascular stents market share by product type. EVAR stands for “endovascular aortic repair.” Values extracted from^[9].

small improvements in PAD treatment could bring about significant differences not only for the patients, but also for the entire health care system.

Angioplasty, also known as percutaneous transluminal coronary angioplasty (PTCA) or percutaneous transluminal angioplasty in peripheral circulation, is an interventional procedure to open narrowed vessels. Balloon angioplasty involves opening the stenosed vessel by inflating a catheter-balloon in the stenosed area. Once the catheter reaches the desired zone, the attached balloon inflates to flatten the atheroma plaque against the artery walls. Subsequently, the device (balloon and catheter) is withdrawn and the vascular vessel remains opened. Balloon angioplasty provides short-term benefits with some improvements in patency.

In stent procedure, on the other hand, VS is placed in the treated area after the flattening of atheroma. VS are cylindrical medical devices acting as endoprosthesis. VS implantation aims to support the walls of a blood vessel during a certain period of time and prevent restenosis. Once the VS is implanted in the desired position, its final scope is to exert permanent pressure against the vessel walls, acting as a scaffold to keep the artery or vein open until the risk of full closure finishes. VS can also be used as flow diversion devices to treat aneurysm. In this procedure, the stent redirects the blood flow and eliminates the pressure on the aneurysm, reducing the rupture risk.

Disregarding the type of intervention, the ultimate objective against atherosclerosis complications is to guarantee blood circulation in the long term after the vessel opening, also referred to as patency. The patency is the state or quality of being open, unblocked, or unobstructed. Even as it seems simple, full patency after angioplasty is still a challenge. Although VS is an innovation in cardiology that has helped saving millions of lives worldwide, they still have some drawbacks and weak points in peripheral vascular disease that require attention.

The present review focuses on the most recent studies using three-dimensional (3D) printing techniques to produce VS, both by itself and in combination with other techniques. Due to the complexity of both disease and treatments/medical devices used, the first part of the review is devoted to the most common types of VS, their characteristics, and production techniques. The paper also focuses on the use of 3D printing (3DP) by reviewing the most recent studies that have approached this technique for the manufacturing of VS. The ultimate aim of this review is to offer a rational overview of the strengths and weaknesses of 3DP in the development of these medical devices, identifying research gaps, possible market niches, and feasible future directions.

1.1. Types of vascular stents and their features

VS have been in use since 1977^[10]. From that moment onward, different aspects concerning VS, such as the type of materials used and the implantation and production technology, have significantly evolved. Any innovation in VS field comes with new challenges arise, either in the manufacturing process or in the final performance of the medical device. The joint effort of the scientific community in the search for the full-patency VS has given rise to the development of a wide variety of cardiovascular stents, which are currently available in the market (Table 1). Figure 2A represents different types of VS depending on their permanence in the human body, the implantation methodology and the therapeutic activity together with their relative presence in the current market (Figure 2B).

Permanent stents or non-resorbable stents are made of materials that do not suffer degradation under physiological conditions. The first VS were bare metal stents (BMS), which were made of stainless steel and nickel-titanium alloy (first-generation stents). It is possible to find cobalt, chromium, platinum/iridium and platinum/chromium, or tantalum BMS^[11]. One of the main inconveniences of BMS are the long-term side effects: although they help to maintain the angioplasty result and they possess excellent mechanical properties, the remaining of the medical device within the vascular vessel could lead to vascular injury, inflammation, thrombosis, and other cardiovascular complications, such as in-stent restenosis in the long term^[8,12]. According to Uhlemann *et al.*, BMS have approximately a 30% chance of restenosis within 6 months^[13]. Moreover, their permanent presence may interfere with future cardiac interventions. The corrosion of metallic VS might accelerate or trigger atherosclerosis as well as release some toxic ions causing long-term inflammatory responses^[14].

BMS can be coated with different substances, aiming to modify their superficial properties and improve their mechanical, biological, and therapeutic performance. Stent surface coating has been used to improve VS biocompatibility and mitigate toxicity. Bearing in mind that the internal part of the stent is in intimate contact with blood flow, they must be fully biocompatible and able to avoid platelet, protein, and other molecules adhesion while maximizing the adherence of specific cells such as endothelial cells. Coating process enables to control and reduce corrosion (oxidation) and the release of undesirable elements or chemicals^[15,16]. The category “coated stents” usually overlaps with “drug-eluting stents” (DES), since organic coatings (mainly polymers such as poly(ethylene), polyurethane, polylactides...) can act as drug reservoirs with controlled drug release properties.

Table 1. Some of the commercialized VS for cardiovascular system classified by material (polymer or metallic) and other important features

Commercial name of the stent	Polymeric	Metallic	Other features			Blood vessel type		
			SE	DES	BRS	Coronary	Peripheral	Aorta
Vascuflex® 5 and 6 F		✓	✓				✓	
Vascuflex® 2-LOC		✓	✓				✓	
Vascuflex® 3-LOC		✓	✓				✓	
Resistant and RESISTANT XL		✓	✓				✓	✓
Xolo™		✓	✓				✓	
Easy Flype		✓	✓				✓	
Easy HiFlype		✓	✓				✓	
Easyflex		✓				✓		
Heliflex TI		✓	✓	✓			✓	
Championir™		✓	✓				✓	
PMSX		✓	✓				✓	
S.M.A.R.T. Control™		✓	✓				✓	
Neuroform Atlas		✓	✓			✓		
E-XL		✓						✓
Acclino® Flex Stent		✓	✓			✓		
Zeus SX		✓	✓				✓	
Jaguar		✓	✓				✓	
Discovery 5F™		✓	✓				✓	
Sinus XL		✓	✓					✓
MC-Peripheral 6F		✓	✓				✓	
Finebent		✓	✓				✓	
LVIS™		✓	✓				✓	
P64		✓	✓			✓		
Biomimics 3D™		✓	✓				✓	
Silkenflex™ Iliac		✓	✓				✓	
Facile		✓					✓	
CGUARD™		✓				✓		
MERES 100™		✓		✓	✓		✓	
MER		✓	✓			✓		
Accero®		✓	✓			✓		
CMCP001		✓						✓
Eucalimus	✓	✓		✓		✓		
ITRIXII	✓			✓	✓	✓		
Desolve™	✓				✓	✓		
Advanta V12	✓	✓					✓	
Fantom®	✓			✓	✓	✓		
Neovas™ Sirolimus-eluting		✓		✓	✓	✓		
Gureater®		✓		✓		✓		
Partner®		✓		✓		✓		
Coroflex® ISAR Neo		✓		✓		✓		

(Continued)

Commercial name of the stent	Polymeric	Metallic	Other features			Blood vessel type		
			SE	DES	BRS	Coronary	Peripheral	Aorta
Coroflex® Blue Neo		✓				✓		
Coroflex® Blue Ultra		✓				✓		
Eurolimus™		✓		✓		✓		
E-Magic® PLUS		✓		✓		✓		
Biomatrix Alpha™		✓		✓		✓		
Biomatrix	✓	✓		✓	✓	✓		
Neoflex™		✓		✓	✓	✓		
CRE8™EVO		✓		✓		✓		
DES-CRE8™		✓		✓		✓		
Titan Optimax		✓		✓		✓		
Helios LD	✓	✓		✓			✓	
Biomime™	✓	✓		✓	✓	✓		
EVERPRO	✓	✓		✓	✓	✓		
MOVYRAP	✓	✓		✓	✓	✓		
TWINRAP	✓	✓		✓	✓	✓		
AVIPLUS	✓	✓		✓	✓		✓	
Xlimus Series	✓	✓		✓	✓	✓		
Orsiro	✓	✓		✓	✓	✓		
Zilver® PTX®		✓	✓	✓			✓	
Dynamx™	✓	✓		✓	✓	✓		
Firehawk®	✓	✓		✓	✓	✓		
Abrax™	✓	✓		✓		✓		
Angiolite BTK	✓	✓		✓			✓	
Bios Expert	✓	✓		✓	✓	✓		
Sequence™	✓	✓		✓	✓	✓		
Yukon® Choice PC	✓			✓	✓	✓		
Decent S	✓	✓		✓	✓	✓		
Pronova	✓	✓		✓	✓	✓		
Intrepide™		✓		✓		✓		
Xplosion+™	✓	✓		✓	✓	✓		
Nile® PAX		✓		✓		✓		
Inspiron	✓	✓		✓	✓	✓		
Cygnus II		✓				✓		
Svelte™		✓				✓		
Arthospico		✓				✓		
Cronus Plus		✓				✓		
Besmooth		✓					✓	
Mguard prime		✓				✓		
Chroma™		✓				✓		
CCFlex		✓				✓		

(Continued)

Table 1. Continued

Commercial name of the stent	Polymeric	Metallic	Other features			Blood vessel type		
			SE	DES	BRS	Coronary	Peripheral	Aorta
Nexgen™		✓				✓		
Twinflex		✓				✓		
Andrastent		✓				✓		
BMS		✓				✓		
Renatural M		✓		✓	✓	✓		
Renatural P	✓			✓	✓	✓		
Magmaris		✓			✓	✓		
Amaranth Fortitude™	✓				✓	✓		
Biofreedom™ Ultra		✓		✓		✓		
Cobra PZF™		✓				✓		
Catania™	✓	✓				✓		
Propass		✓				✓		
Nano+™		✓		✓		✓		
Eluvia™	✓			✓			✓	
Epic™		✓	✓				✓	
Express™ LD		✓					✓	
Express™ SD								
Innova™		✓	✓				✓	
Promus PREMIER™	✓	✓		✓		✓		
Promus ELITE™	✓	✓		✓		✓		
SYNERGY™	✓	✓		✓	✓	✓		
REBEL™		✓				✓		
SYNERGY™ XD	✓	✓		✓	✓	✓		
SYNERGY MEGATRON™	✓	✓		✓	✓	✓		
Zilver®		✓	✓				✓	
Zilver® Vena™		✓	✓				✓	
Zilver® PTX®		✓		✓			✓	
Magmaris® RMS	✓	✓		✓	✓	✓		
Orsiro Mission	✓	✓		✓	✓	✓		
PRO-Kinetic Energy		✓				✓		
PK Papyrus		✓				✓		
Astron		✓	✓				✓	
Astron Pulsar		✓	✓				✓	
Pulsar-18		✓	✓				✓	
Pulsar 18 T13		✓	✓				✓	
Pulsar-35		✓	✓				✓	
Dynamic		✓					✓	
Dynetic®-35		✓					✓	
Dynamic renal		✓					✓	
iVolution		✓	✓				✓	
Restorer		✓					✓	

SS, stainless steel; SE, self-expandable; DES, drug-eluting stent; BRS, bioresorbable.

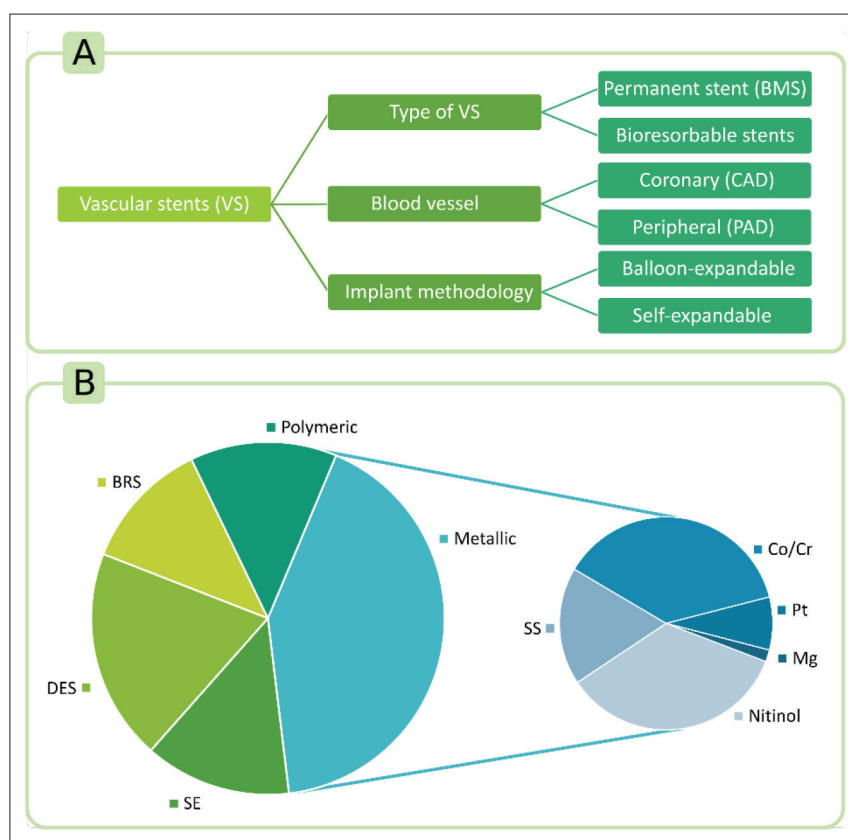


Figure 2. (A) Classification of VS based on their degradability, type of blood vessel (to treat CAD or PAD) and implantation methodology. (B) Relative amount of VS commercially available in the market. BRS stands for “bioresorbable stents,” SS “stainless steel,” SE “self-expandable stent,” and DES “drug-eluting stent.” The sector graph is drawn according to the information available in Table 1.

Bioresorbable (BRS) VS are made of biodegradable materials, which can be degraded over time under physiologic conditions until total disappearance. For a proper functioning, total BRS VS degradation must occur at a desirable, predictable rate, leaving behind a native vascular vessel fully repaired^[15,17]. In fact, the control and prediction of their biodegradation rate is still the main challenge in the production and improvement of this group of VS. Despite some exceptions such as BRS metallic stents made of Mg, Ti, and Zn, biodegradability is a property usually associated to substances and molecules with poorer mechanical properties than metals (polymers). This means that the major part of the ingredients used for the production of BRS VS undertake poorer mechanical support when compared with BMS^[12].

DES are VS that carry active substances in their structure, which are progressively released to obtain a certain therapeutic effect. DES prevent or reduce some of the BMS side effects: thrombosis, neointimal scar tissue formation, restenosis, etc. In addition to the main active substances loaded into DES, other substances also include antithrombotic drugs (heparin), antiproliferative

(paclitaxel, actinomycin D), immunosuppressive (sirolimus) and anti-inflammatory (dexamethasone) drugs^[18]. The use of paclitaxel has been particularly useful in the prevention of in-stent restenosis according to [8]. Recently, the review of Beshchasma *et al.* has reported that nanoparticles and genes can also be loaded into DES^[15]. Therefore, DES are considered Modified Drug Delivery Systems (MDDS) since they must protect, carry, and control drug release toward the vessel walls or the bloodstream. These medical devices are commonly made of drug-polymer coating or direct drug immobilization on the stent surface^[15,18]. The most common techniques to load drugs on stent struts are spray coating and dip coating. Regarding spray coating, a nozzle, which creates droplets of approximately 10 μm in diameter, sprays the drug solution or drug/polymer composite solution over the stent struts. For dip coating, the whole stent is dipped into the drug or drug/polymer solution in repeated occasions. The excess of material over the stent is then removed by spinning or other techniques^[19]. DES can be differentiated into first and second generation or third generation, with the former one including non-bioresorbable DES and the latter one belonging to BRS DES^[15].

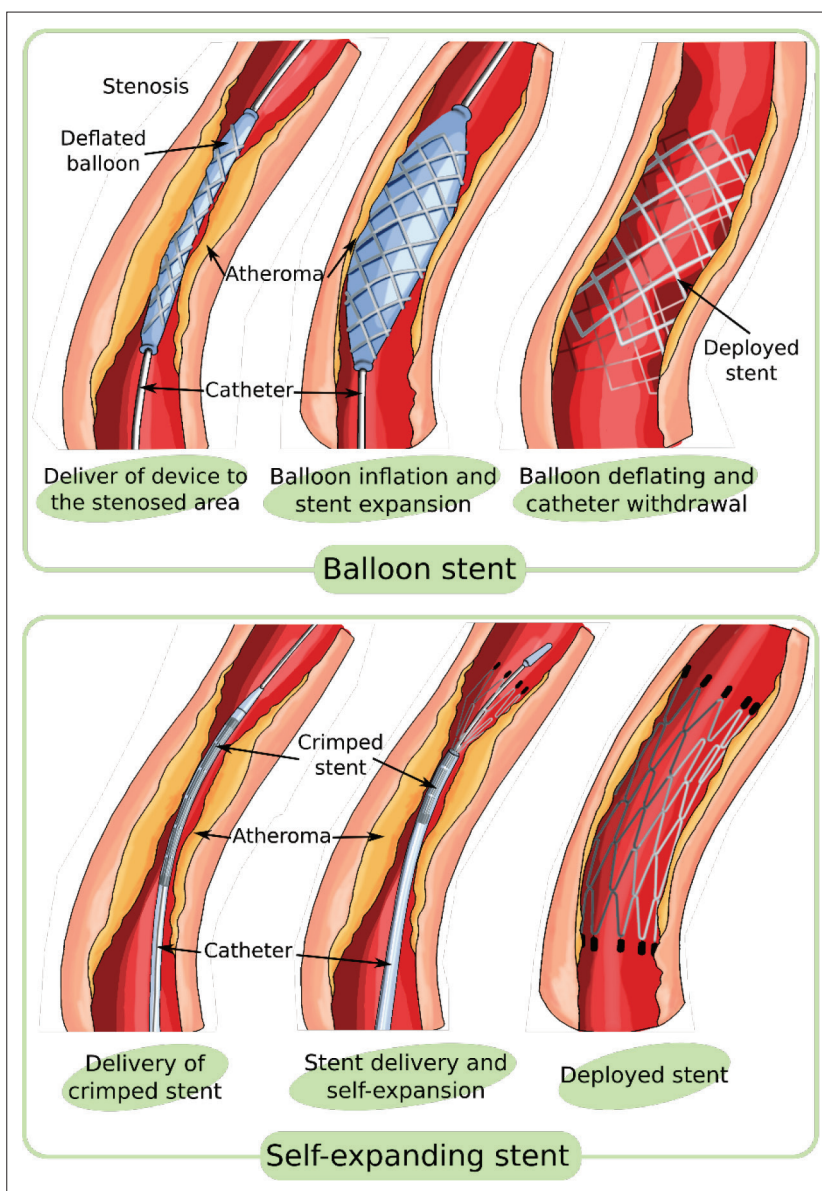


Figure 3. Schematic representation of VS implantation procedures. Top: balloon-mediated stent delivery; bottom: self-expanding stent delivery.

Stents can also be differentiated by the implantation procedure, which is designed depending on the particularities of the stent itself. Balloon expandable stents are transported to the desired zone mounted around an inflatable device called “balloon.” Once in the desired area, the balloon is inflated until a certain point, forcing the stent to expand to the desired dimensions and guaranteeing the opening of the vessel (Figure 3, top). The corresponding counterpart are self-expandable stents, which are also transported with a catheter to the desired area. Nonetheless, in this particular case, the stent is crimped inside a thin tube that deploys it once in the correct position (Figure 3, bottom). That is, self-expandable

stents are able to expand on their own, due to their high radial force, whereas balloon-expandable stents must be dilated to be implanted. Each placement strategy demands different stent mechanical properties and geometries. As stated by Krankenberg *et al.*, “whereas self-expanding stents are of high elasticity but apply low radial outward force, balloon-expandable stents are rigid but support high radial outward force and allow to be placed with greater precision”^[20].

Finally, VS can also be differentiated based on the type of blood vessel: peripheral or coronary (Figure 2A). The significant success of coronary stenting has encouraged the translation of this technology to the treatment of PAD

Table 2. Differential properties and features of peripheral and coronary blood vessels influencing the patency of PAD and CAD stenting

Differential characteristic	Coronary blood vessels	Peripheral blood vessels
Blood flow	Excellent autoregulation (60–200 mm Hg) to maintain normal blood flow under aortic pressure changes ^[24] .	Moderate autoregulation (50–70 mmHg). Stenosis could reduce distal pressures below the autoregulatory range causing maximally dilated vessels and further pressure reductions ^[25]
Blood oxygenation	Flow tightly coupled to oxygen demand due to high basal oxygen consumption by heart ^[24] .	Moderate pressure autoregulation could lead to tissue hypoxia.
Extent of the stenosed lesion	Smaller, localized lesions.	Much longer lesions, usually located between muscle and bone.

that affects peripheral blood vessels, such as femoral, iliac or popliteal arteries, among others^[21]. In fact, the endovascular treatment of PAD still yields unsatisfactory patency rates^[22] or no significant differences between stenting and percutaneous transluminal angioplasty (PTA) in the lower extremities^[23]. Among subjects with diabetes, the risk of PAD is often severe and associated with extensive arterial calcification, thus leading to a particular type of lesion that could complicate the stenting procedure. Definitely, PAD and CAD respond differently toward the same pathology and intervention, due to differential features and characteristics summarized in [Table 2](#). The differential anatomy of coronary and peripheral arteries (size, bifurcations, elasticity, and curvature) influences the shear stress and blood turbulences, indicating the need to adjust the VS to the idiosyncrasy of each vessel. The blood flow and blood pressure and perfusion is better regulated in the heart due to excellent autoregulation mechanisms of these vessels, thus guaranteeing optimal blood flow^[24]; on the other hand, other organs such as skeletal muscle and splanchnic circulations show moderate autoregulation^[25]. If blood pressure drops to below the autoregulatory range due to pathologies such as stenosis, the distal vessels will be maximally dilated in an attempt to guarantee proper blood flow, thus causing further pressure reductions. When stenting peripheral blood vessels, the moderated autoregulation of blood pressure and flow could hinder the function of the vessel in maintaining the open lumen. Because of this, stents with better radial force are desirable for PAD. Another factor to bear in mind is blood oxygenation of the tissues in the distal region of the stenosed vessel. When it comes to the heart, the flow is tightly coupled to oxygen demand (when cardiac O₂ consumption increases, there is an increase in coronary blood flow)^[24], indicating that it is more easily compensated in CAD. In the case of PAD, the moderated pressure autoregulation of the peripheral tissues could lead to oxygen-starvation of the distal tissues as well as inflammation, hypoxia, edema, ulceration, and, ultimately, amputation in the long term. The lower blood oxygenation in PAD worsens the prognosis of the treatments, including stenting. Another

factor to consider when designing and implanting a stent is the extent of the stenosed lesion: in CAD, normally the size of the stenosed area is smaller and more localized (always with exceptions), while in PAD, the lesions can be much longer and usually located between muscle and bone tissue. The lesion size and its location imply that the stent will be subjected to higher level of movements and stresses (e.g., displacement, fracture, crushing). Therefore, more flexible VS are preferred for PAD, while the VS is allowed to be a little stiffer for CAD because it will not be subjected to so much movements.

2. Desirable stent features

In general, the perfect VS has the ability to be crimped in agreement with the implantation methodology (balloon or self-expansion), and has good expandability ratio with enough radial strength and minimal recoil. VS must also be flexible and fully biocompatible, as well as able to prevent or avoid thrombosis and restenosis after implantation^[26]. These desirable properties and features are intimately related to the stent raw materials, their combinations, and the intrinsic features of each of them as well as the manufacturing process and post-processes. Nevertheless, the geometry and design of the VS are likewise important to control the final properties of the medical device, including the mechanical properties^[27]. Under these circumstances, the study of the geometry and dimensions of VS is a field of study on its own due to the myriad of possibilities. In this sense, computational studies have proven themselves as useful tools to analyze and predict the influence of stent design on the final performance.

Good expandability is the property of a material to expand (active expansion or self-expandability) or to be expanded (passive expansion). VS implanted with a balloon are passively expanded by the inflation of the balloon. Therefore, the materials used for the manufacturing of balloon-expandable stents need to be more plastic than elastic. On the contrary, self-expandability of VS refers to the ability of the medical device to expand without the use of an external force and to retain the final shape. This can

also be known as “elastic memory.” Self-expandable stents are fabricated in their expanded shape (final shape) and subsequently crimped into the delivery system (catheter). Apart from self-expandability, these stents should also possess low elastic modulus and high yield stress for large elastic strains. The elastic modulus measures the resistance of the material to elastic deformation. Low moduli materials stretch a lot when pulled, then recovering their original shape. The elastic strain is the amount of deformation of a material that is fully recovered upon removal of the stress without any residual plastic deformation. Recovery elastic deformations around 10% are considered large elastic strains and thus suitable for the manufacturing of stents. The major part of self-expandable stents are made from braiding, knitting or tubing^[28].

Radial strength is the strength needed to compress a material (a VS in this particular case). Proper radial strength of VS is of great importance because it will determine the permanence of the stent in position and its ability to maintain the vessel properly open (patency), which is of special importance in PAD. That is, a VS must possess enough radial strength to hold the vessel and to prevent migration of the medical device. On the contrary, excessive radial strength may lead to vessel overexpansion, causing endothelial injury, inflammatory reaction, and rupture/deformation risk (pseudoaneurysm, dissection). According to Lachowitz, the “structural design of the device plays the largest role in a device’s radial strength and stiffness”^[27]. Briefly, the wider and more open the structure of the VS, the lower the radial strength.

An optimal VS must possess optimal axial flexibility and radial rigidity to guarantee the stent patency. The greater the radial stiffness of the medical device, the greater the pressure exerted over the vascular wall, thus guaranteeing blood flow. On the other hand, the higher the axial flexibility, the better the stent adaptation and deformation to the human body curvatures and less damage to the vascular walls. Solving these two contradictory and coexisting problems of axial flexibility and radial rigidity is one of the main challenges in the design of stents.

VS recoil is defined as the difference between the minimum diameter of the crimped stent (before implantation) and the minimal luminal diameter of the stent after implantation (once expanded). Consequently, recoil stent events affect the lumen diameter and thus the expansion of the stent. This modification could lead to malposition and restenosis. The VS, which is able to maintain its initial expansion diameter, would have lower recoil value and better stent patency in the long term^[29]. Acute recoil is defined as the difference between the maximum diameter of inflated balloon and the diameter

of the VS right after balloon deflation. Cumulative recoil is also used to evaluate the performance of VS, which is the difference between the diameter of VS during balloon inflation and the diameter of the stent lumen 24 h after implantation. The recoil behavior of a medical device can be predicted by quantifying its elastic modulus: the higher the elastic modulus, the lower the stent recoil^[28].

Stent thrombosis is an acute thrombotic occlusion of a coronary VS. Although it may be clinically silent, stent thrombosis is usually associated to acute coronary syndrome symptoms. With respect to stenting in PAS, the thrombotic events can also happen, though later in time. Even if the highest risk falls into the first month after stent implantation, thrombosis could also happen years after implantation, especially for permanent and peripheral VS. Another occlusion of VS happens after neointimal proliferation, which progressively narrows the stent lumen, representing a long-term side effect (6–12 months after implantation and depending on the type of VS)^[30]. In this case, the most frequent sign is the appearance of anginal symptoms (in coronary) or claudication/ischemic (in peripheral) symptoms^[31]. Antiproliferative drugs such as sirolimus, everolimus or paclitaxel are of great usefulness in the prevention of this side effect, especially when locally released from DES.

The evolution of the VS, the implantation procedure and the prophylactic treatment (typically involving the use of two antiplatelet drugs) have allowed for a reduction in the thrombosis incidence, though it is still a matter of concern in this type of interventions. Moreover, Modi *et al.* have reported that there was no significant difference between the rate of stent thrombosis between bare-metal stents and eluting drug stents, and only the timing of the event varies^[31]. Generally, thrombosis is more likely caused by DES, whereas BMS are more associated to in-stent restenosis events. Nonetheless, it is challenging to separate both cases, since they are related to each other in terms of the pathological mechanisms. According to Reejhsinghani and Lofti, delayed arterial healing following DES implantation is characterized by a lack of complete re-endothelialization and persistence of fibrin when compared with BMS, and this delayed healing is the primary substrate underlying all cases of late DES thrombosis^[32]. Since polymer-coatings are commonly applied in DES to control drug release, any hypersensitivity to these ingredients could improve the risk of thrombosis. Once again, the geometry of the stent plays an important role, since it has been demonstrated that thick-strutted stents possess higher thrombotic risk than thin-strutted VS^[33]; therefore, it is necessary to optimize not only the manufacturing, the composition and the implantation strategy, but also the structural design of the medical device.

The optimization of BRS VS manufacturing and features could be the answer to thrombotic and in-stent restenosis issues. The “disappearance” of the medical device, leaving behind a completely restructured, opened and healthy vessel would completely eliminate the long-term complications. It is, therefore, logical to observe that the majority of the current scientific literature on VS is focused on the formulation, manufacturing and optimization of BRS medical devices.

The biocompatibility is related to the immunological response that the VS could cause in the host after implantation. A biocompatible medical device, by definition, does not produce toxic or immunological response when implanted or put in intimate contact with body fluids. In other words, after the implantation of biocompatible VS, the surrounding tissues “accept” the medical device without triggering allergic or inflammatory responses (nor acute neither chronic) as well as in the total absence of toxicity (including carcinogenicity)^[34]. As wisely highlighted by Cvrček and Horáková, the biocompatibility is a concept that not only depends on the chemical and superficial composition of the device, but also on its interaction with the surroundings, the period of the implant application, the mechanical properties (adaptable to the mechanical properties of the host tissue) and the dimensions and shape of the VS^[35]. Biocompatibility tests can be performed either *in vitro* or *in vivo* and are crucial to determine the safety of both the materials and the final device. To maximize the comparability between biocompatibility results among laboratories and industries, the International Standard established normalized biocompatibility studies for medical devices (ISO 10993-5).

3. Production techniques for the manufacturing of vascular stents

The most frequently used manufacturing techniques for the production of VS are braiding, knitting, micro-injection molding and laser cutting. The use of each of them depends on the materials and type of medical device under production. Additionally, other less commonly used methods, such as micro-electrical discharge machining, micro-photochemical etching, water jet, chemical vapor deposition (CVD), magnetron sputtering, and micro-precision milling, have also been employed^[12,28]. Depending on the manufacturing method used, the materials and the final VS features, an additional post-processing step might be required, including drug-coating, surface modification, and surface microstructure^[12,36,37].

The braiding technique produces mesh-like VS by winding wires (with one or more than one material) around

a cylindrical mold called carrier. The wires are braided along the carrier axis of rotation. At the end of the braiding step, the carrier is removed from the braids. Consequently, the dimensions of the resultant VS will mainly depend on the diameter and length of the carrier, although the materials and braiding pattern are also determinants^[12,38]. Inert metals and some polymers are prone to be braided due to their higher mechanical resistance^[39,40]. This manufacturing method is currently underused due to the lack of radial strength presented by braided VS.

Micro-injection molding is a manufacturing process involving high temperatures and pre-formed molds. Generally, the VS material must be liquefied (melted) to be injected into a mold with the desired final shape. After cooling (solidification), the VS is unmolded and released. In this manufacturing technique, biocompatible polymers are the most commonly used materials. According to the recent review of Gao *et al.*, micro-injection molding is widely used for the production of VS, only outpaced by laser-cutting^[12].

Laser-cutting can be envisaged as the contrary of additive manufacturing, since it involves the elimination of excessive material from an original piece until the desired shape remains. To do that, a high-power laser beam focuses on the original material piece (frequently a hollow, tubular piece) to cut it by melting, ablating or vaporizing the irradiated area. Then, the cut piece is eliminated by high-speed airflow^[12]. In this process, the laser beam is immobile, while the moving piece being the tubular, hollow piece of material, which is attached to a rotating axis, are mobile in *x*, *y*, and *z* axes. After laser-cutting, deburring and polishing post-processes are usually required.

Despite the continuous evolution of medical devices, none of the currently available VS guarantee all the desirable features and they are unable to achieve full patency. Suboptimal stent sizes and possible malposition is probable due to inaccurate and limited and pre-established VS dimensions and shapes. In this regard, the production of artificial, individualized stents according to the dimensions, shape, and requirements of each patient would reduce vessel injuries, inflammation, restenosis risks and other complications. It is at this point that 3DP comes into play.

3DP is a manufacturing technique that creates a physical, 3D piece from a digital design (also known as computer-aided design) and adds the material layer-by-layer. The major advantage of 3DP is the versatility of material production and the possibility of easily modify the dimensions or the shape of the resultant piece just by changing the digital design to be printed. Furthermore, the different types of lesions together with the different requirements of VS for treating CAD

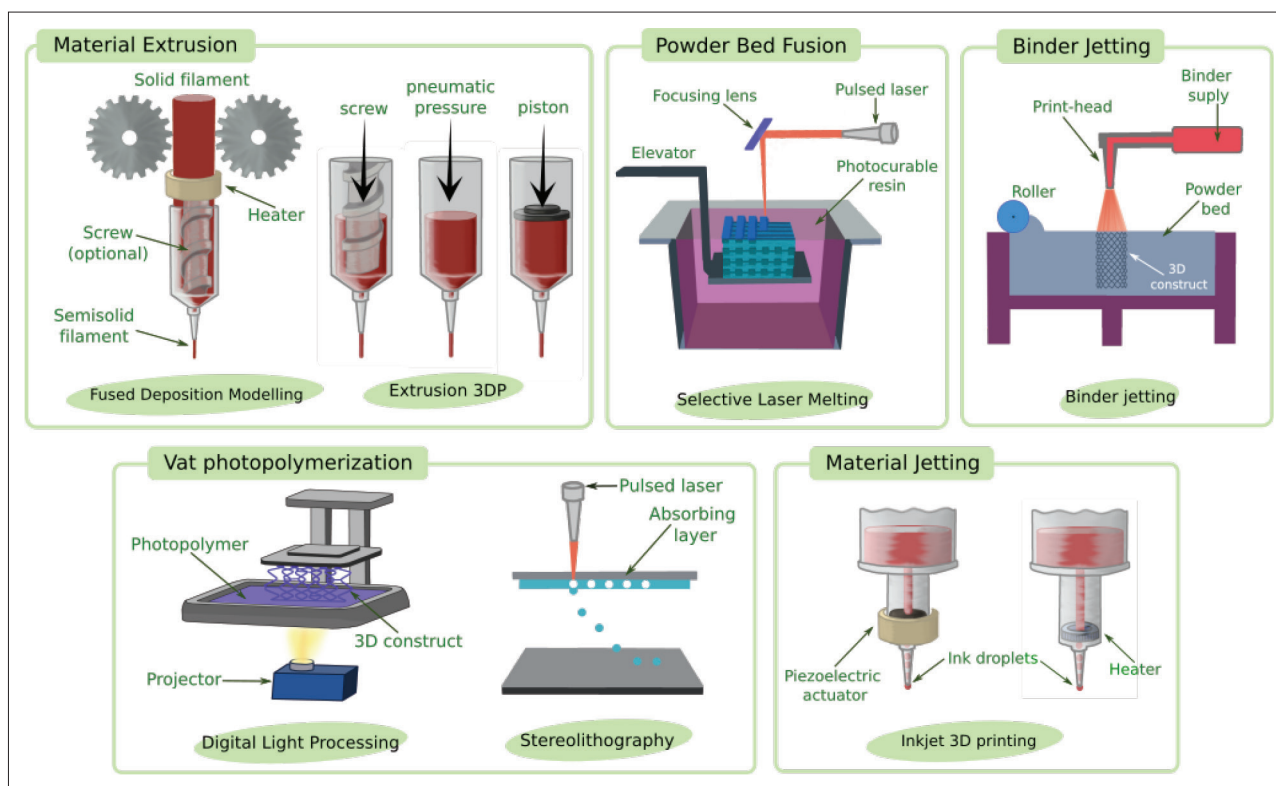


Figure 4. 3D printing techniques classified based on their additive manufacturing mechanism (ISO/ASTM 59000:2021).

and PAD make 3DP a very promising technique because it allows the production of totally personalized VS that takes into consideration not only the dimensions and size, but also the mechanical properties of the medical device^[12]. Apart from the production of tailor-made stents, 3DP is able to translate the computerized image of the patient lesion into a real 3D structure (commonly known as “phantom”), which is useful to guide the surgeon in choosing the most adequate operation, optimal endovascular prosthesis for the patient, physiological simulations, benchtop experimentation, etc.^[41-47]. Likewise, 3DP can be combined with other production methods to upgrade them. For example, different 3DP techniques can serve for the rapid, tailor-made printing of a sacrificial mold from which to obtain the desired medical device; another example, which has already been presented in the literature, is the use of 3DP as a technique to control stent coating, drug release and biocompatibility.

To top it off, 3DP is also a very versatile technique since it allows to use a wide variety of materials and production methods. A brief compilation of the different 3DP techniques will follow, generally classified by following the ISO/ASTM 59000:2021 terminology, and schematically presented in Figure 4.

- (i) Material extrusion (MEX) 3DP is a pressure-driving 3DP technique through which the ink is propelled

through a nozzle either by mechanical (axial piston or screw-driven) or pneumatic forces (air flow) (Figure 4)^[51].

- Air-flow MEX is one of the most commonly used methods for semisolid inks. In this extrusion method, air flow propels the ink through the nozzle^[51,52].
- For those semisolid inks with high viscosity values, screws can be used to propel the ink inside the cartridge in screw-driven MEX. They can be used on their own (for semisolid, high-viscosity formulations) or can be used as additional propelling systems in other 3DP techniques such as fused deposition modeling.
- Fused deposition modeling (FDM) consists of melting of thermoplastic materials, which are subsequently extruded through a temperature-controlled extrusion print-head that turns them into a semisolid state. The materials are fused as they are deposited due to temperature drop, thus creating a 3D structure. Among the most used thermoplastic polymers, PCL, PLA and PLLA should be highlighted. Due to the nature and properties of these materials, FDM allows for the creation of durable 3D constructs. The

main limitation of this technique regarding tissue engineering and bioprinting of artificial tissues or medicines is the high temperatures of the majority of thermoplastic polymers, which are incompatible with the stability of drugs, cells and a wide variety of biological ingredients^[48-50]. Nonetheless, owing to the required properties and features of VS, FDM allows the production of tough and resistant 3D constructs, thus accomplishing the optimal mechanical properties of these medical devices.

- (ii) Vat photopolymerization (VPP) embodies all the techniques in which a “liquid photopolymer in a vat is selectively cured by light-activated polymerization” (ISO/ASTM 59000:2021). In the field of 3DP, digital light processing (DLP) and stereolithography (SLA) (Figure 4) can be differentiated. Both of them use laser-based liquid resin polymerization technology, differing in the light source and the curing methodology employed: SLA utilizes a mobile UV laser beam while DLP works with UV light from a static projector. In DLP, the UV light remains stationary, and the entire liquid receives light with a single projection of the structure to be printed; in SLA, the laser beam moves while tracing the geometry layer-by-layer^[50]. Therefore, DLP is faster than SLA, though the precision and accuracy can be compromised for too complicated structures. Another remarkable difference to bear in mind, especially when it comes to scale-ups, is the production costs, since SLA printers are more expensive than DLP.
- (iii) Material jetting (MJT) 3DP technique is also known as “drop-on-drop deposition,” “droplet-based 3DP” or “inkjet 3DP” (Figure 4). It is a non-contact printing technique that reproduces the 3D design by selectively depositing droplets of the so-called “ink.” These droplets can be created by different techniques such as thermal, piezoelectric or electrostatic actuators. MJT 3DP can also be divided into continuous or drop-on-demand, depending on the frequency of ink drop ejection^[19,52-54].
- (iv) Powder bed fusion (PBF) 3DP is also known as selective laser melting or selective laser sintering (Figure 4). It consists on fusing metallic powders by melting them with a high power-density laser. PBF enables the generation of 3D scaffolds with superior geometrical freedom in comparison to other 3DP techniques. Among the most used materials for this technique, aluminum, titanium,

copper, chromium, cobalt chromium, stainless steel, and super-alloys should be mentioned. After the deposition of a thin, uniform layer of powder, the laser scans the desired shape to induce melting and fusion of the material, thus binding the powder particles to create the 3D construct^[55-57]. This 3DP technique is usually associated to rough surfaces in the final 3D constructs, which is undesirable when it comes to VS^[37]. Therefore, the use of PBF necessitates post-processing techniques (such electrochemical polishing) to smoothen the construct’s surface.

- (v) Binder jetting (BJT) 3DP is also known as “drop-on-solid deposition,” “drop-on-powder,” “drop-on-bed sedimentation,” “binder jetting,” or “plaster printing”^[50]. BJT is a non-contact 3DP technique based on the spreading of a solid material (often powder) followed by a liquid linker or binder (Figure 4). The liquid binder, deposited in the required areas, binds the powder and increases its consistency layer-by-layer, thus creating the 3D structure.

Solvent-casting 3DP (SC-3DP) is midway between PBF and MEX 3DP techniques. Depending on the type the materials used, they can be classified as extrusion-based 3DP or as powder-solidification 3DP. In SC-3DP, the solid material and its proper binder are mixed in the same cartridge, that is, the powdery material (either metal or polymer) is mixed with its proper binder system (i.e., polymers, volatile solvents, etc.) and extruded through a nozzle. Post-processing steps such as debinding and sintering techniques are needed afterward^[58]. Debinding refers to the elimination of unnecessary additives (such as binding polymers). Sometimes, this step consists of solvent evaporation in an open environment. A sintering process is the binding or “coalescence” of a solid mass by means of heating or compression, and a post-processing step, which can be overlooked for most polymers, is usually necessary for strong materials such as metals.

4. 3D printing for vascular stents

Although all 3DP techniques are based on the same principle, there are significant differences between them that significantly affect the employed materials, the printing procedure and the final properties of the 3D construct. In other words, not all the 3DP techniques are suitable for the production of every VS, and not every material is compatible with all the 3DP processes. In view of this, it seems logical to address the available studies in view of the 3DP technique used in each case so as to gain a more comprehensible understanding about the strong and weak points of each technique.

4.1. Material extrusion 3DP as vascular stents manufacturing technique

Thermoplastics are a wide group of synthetic materials with versatile properties (flexibility, pliability, thermoresponsive) and acceptable mechanical strength. Some of them are biodegradable and biocompatible and have high value properties in the manufacturing of medical devices. Due to their polymeric nature, thermoplastics have proven to be useful drug carriers and delivery systems. In the particular case of 3DP, thermoplastics are optimal feedstock for FDM due to their ability to acquire semisolid, viscous consistency at high temperatures and recover solid state after cooling, whereas in the VS field, thermoplastics' thermoresponsive behavior makes them valuable ingredients in the production of self-expandable VS.

Polycaprolactone (PCL) and polylactic acid (PLA) have been used to formulate an ink for FDM printing^[59,60]. The stent composition and different BRS geometries in the final properties have been explored, including the effect on cellular proliferation. To understand the results and optimize the 3DP process, PCL stents were printed onto a computer-controlled rotatory platform under different conditions (nozzle temperature, fluid flow rate, printing speed)^[60,61]. The printing temperature and flow rate were the factors reporting the strongest influence over PCL printability. The increase in the printing speed reduced the PCL cooling rate, changing the final properties of the material. This was ascribed to a more effective heat dissipation^[61]. In another study dealing with PCL and PLA, pure PCL showed 35% higher fibroblast proliferation than pure PLA stents, which was attributed to the different molecular weight of both ingredients (smaller molecular weight usually lead to lower cellular proliferation). Despite that, the mechanical properties revealed that the combination of PLA and PCL was the most appropriate for a stent due to the combination of PCL elasticity and PLA rigidity: the former prevents PLA breakage during stent expansion, while the latter hindered PCL recoil after placement. The use of PCL in the external wall of the BRS VS has been proposed to increase endothelial cells proliferation, while an internal PLA wall will help to retain cellular proliferation and prevent restenosis^[59]. In another study, PLA and polyvinyl alcohol (PVA) were combined and 3D printed into a BRS VS with an arrow-like geometry, providing negative Poisson's ratio or in other words, an auxetic structure^[62]. Auxetics are structures with high energy absorption and fracture resistance. The complexity of this geometry was accurately achieved through FDM by the combination of these two ingredients, in which PVA is merely acting as a temporal support during the printing process: after being printed, the water dissolution of PVA leaves a final, solid stent made of PLA (Figure 5,

top). The auxetic geometry maximizes the stent anchorage with vessel walls, thus minimizing the risk of malposition and displacement. Different diameters, lengths and dimensions of the final stent were tested to obtain the best mechanical features (Figure 5, bottom). These studies revealed that for this particular geometry, the higher the stent diameter, the lower the radial force provided by PLA. Additionally, the higher the wall thickness, the better the compressive properties. Thus, PLA is a good material for the production of small-diameter stents with considerable wall thickness and good recoverability, which are the features that guarantees the correct placement of the medical device^[62]. The feasibility of PLA as VS raw material has also been confirmed by Jia *et al.*^[63] In this case, PLA stent produced with FDM maintained its excellent shape at room temperature during 1 week storage, and only recover the original shape within 5 seconds after being exposed to 70°C^[63]. The necessity of such a high temperature to trigger VS expansion (70°C) implies the necessity of applying heat into the implantation area. Given that, the term "self-expansion" is subjected to discussion, since external stimuli is still needed for the implantation of these stents. Temperatures closer to the human body are needed for these stents to be entirely "self-expandable" in order to obviate the need of external stimuli during deployment.

FDM was also used to print a stent made of PCL with a rotary mandrel, which is subjected to voltage^[36]. This 3DP machine is somewhat based on electrospinning technology. The raw PCL was shaped as particles that must be transformed into filaments to enable 3DP. To do so, PCL particles are melted in a heating chamber associated to the printer, and subsequently transported to the extruder needle, which deposited them in a rotatory mandrel subjected to an electric voltage (4 kV). This 3DP technique made the fabrication of small stents with remarkable resolution and reproducibility possible^[36].

In another study, the acrylated, photocurable, and thermoresponsive polymer PGDA (poly(glycerol dodecanoate acrylate) was deposited at 45°C to produce an easily implantable stent (Figure 6B)^[64]. The intrinsic properties of its precursor (PGD) together with the photocurable ability of PGDA allowed the printing of 3D-tilted structures without collapsing (Figure 6A). Good biocompatibility and cellular adhesion and proliferation were observed after the implantation of the 3D-printed VS in a mouse aorta (Figure 6C). Endothelial cells, adipocytes and connective tissue adhered and proliferated around the stent within just 14 days^[64].

The intervention of a stenosis is rather complicated if it happens in a bifurcated vessel. In such a case, two different stents are used (one for each branch) and then,

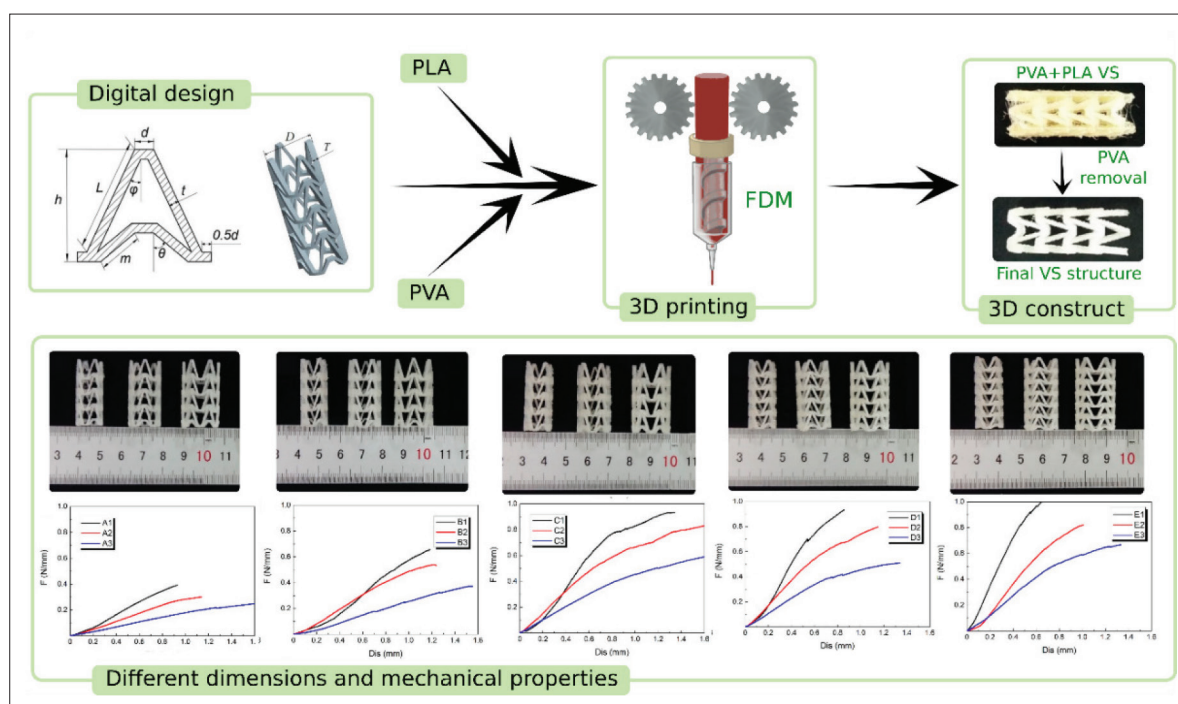


Figure 5. Combination of PLA and PVA for the production of VS by means of FDM 3DP. PVA was included as a sacrificial material allowing the printing of a self-standing structure. After the printing process, PVA was dissolved and eliminated, revealing the final VS structure, which is made of PLA. The influence of stent diameter, wall thickness and geometric parameters of the auxetic structure were studied, and different printed VS and their mechanical properties were evaluated. Graphics included in the figure correspond to radial force (per unit length) versus radial displacement curves for each stent. Reproduced with permission from [62] 2018, *Materials*.

they are joined at the confluence area. Therefore, for each vessel branch, an additional surgical procedure is needed. Moreover, the diameter, shape and/or type of lesion can also be different in each branch, further complicating the intervention. FDM 3DP was successfully used to obtain a one-piece, bifurcated stent (y-shaped) made of thermoplastic polyurethane with the optimal geometry for each case^[65,66]. To top it off, the printed stent possesses two different geometries that are able to crimp and deploy the full stent in the bifurcated vessel in just one step. The synthesis of one-piece stents housing more than one geometry and different dimensions is not feasible with other techniques. So, 3DP is a robust and promising method to address these particularities.

Sirolimus is an immunosuppressive active substance indicated after transplantation or implantation of organs/devices. This drug has been included in a BRS VS made of high-molecular-weight poly (L-lactic acid) resin (PLLA), a common ingredient in the production of vascular stents^[67]. PLLA is a biocompatible, biodegradable and crystallizable thermoplastic, enabling 3DP through FDM. The final properties of the sirolimus-loaded BRS produced by FDM 3DP were assessed. The printing process was carried out at 210°C, extruding

the melted PLLA over a computer-controlled rotatory platform. The resultant stent exhibited good mechanical properties both before and after gripping and expansion, suggesting that it could maintain effective radial strength even after long-term degradation. Sirolimus was released in a controlled manner for 18 months.

Another strategy to apply 3DP to the production of stents involves using the printer to obtain a 3D negative mold of the stenosed area to be treated, on which the stent is produced or shaped. This strategy, which is known as rapid prototyping sacrificial core-coating forming (RPSC-CF), has been recently proposed for the synthesis of a metal-polymeric aortic stent graft^[68]. They fabricated a 3D water-soluble core by FDM. This mold was subsequently dipped in polyurethane (PU) dissolved in THF (imidazole and tetrahydrofuran) (Figure 7A), and the metallic part was placed (nitinol wires, Figure 7B) and wrapped in the inner coating surface of PU solution. The final dissolution of the 3D-printed core signified that the metal-PU stent was ready for implantation (Figure 7C). After 30 days of *in vivo* implantation, authors reported that the stent stayed put (without displacement) and effectively supported the aorta walls. The fabrication of this personalized stent graft can be achieved in 3–4 days^[68].

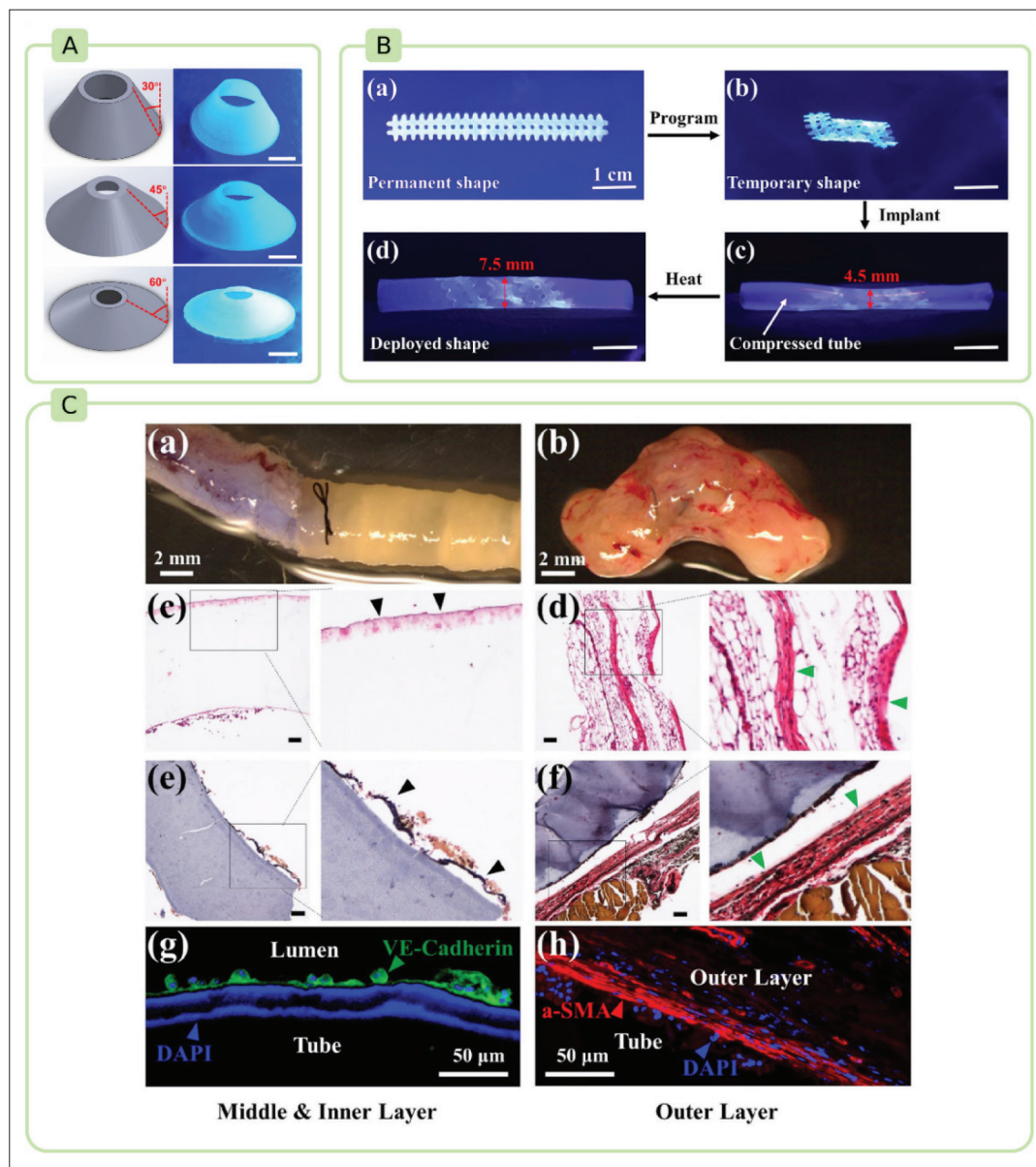


Figure 6. (A) Tilted structures printed (scale bar: 1 cm). (B) Steps of *in vitro* deployment testing. Different frames, from (a) to (d), show the shape memory effect of PGDA after photocrosslinking and thermal curing. Effective deployment inside a compressed silicone tube. (C) Results of *in vivo* studies in mouse aorta; (a) images after implantation and (b) after 14 days; (c), (d), (e), and (f) correspond to different staining techniques of middle/inner (c and e) and outer layers (d and f) of newly formed tissue after 14 days of VS implantation. Black arrows indicate inner elastin layer and green arrows indicate outer elastin layer; (g) endothelial cells stained with VE-cadherin antibody (green) and cell nuclei stained with DAPI (blue); (h) myofibroblasts (red) and nuclei stained with DAPI (blue). Reproduced with permission from [64] 2021, *Acta Biomaterialia*.

Other MEX-based studies have also been reported feasible methodologies for printing VS, even if these techniques depend on semisolid-like materials. Some plastic materials can be dissolved in certain solvents that left behind a solid structure after evaporation. Particularly, PCL, PLGA, and polyethylene glycol (PEG) were dissolved, extruded and subsequently coated with sirolimus by means of ultrasonic spray method^[69]. This 3DP methodology enables the production of a helical, biocompatible BRS and

DES with successful results *in vivo* and *in vitro*. Sirolimus-coated BRS was able to reduce neointimal hyperplasia in male pigs for 4 weeks compared to the corresponding counterpart without sirolimus, together with reduced thrombosis and inflammation. This effectiveness has been related to the controlled release of sirolimus for 31 days. It is also worth to mention that the *in vivo* stent implantation was performed without much complications, proving that 3DP stents are suitable for real treatments. MEX 3DP has

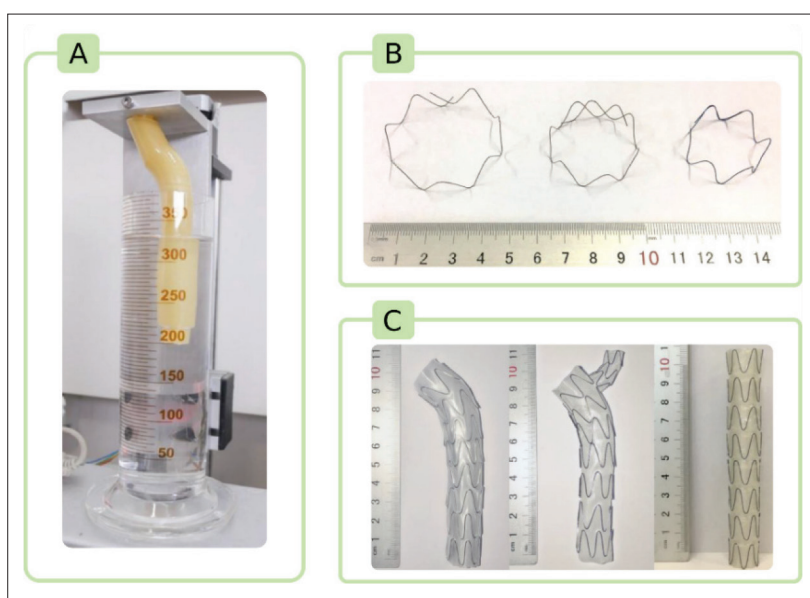


Figure 7. (A) Pulling platform for deposition process over the sacrificial mold obtained by means of 3DP. (B) Shaped nitinol wires to be used in the final stent. (C) Final aspect of aortic metal-PU stents with different shapes (branched and straight). Reproduced with permission from [68] 2020, *Medical Engineering and Physics*.

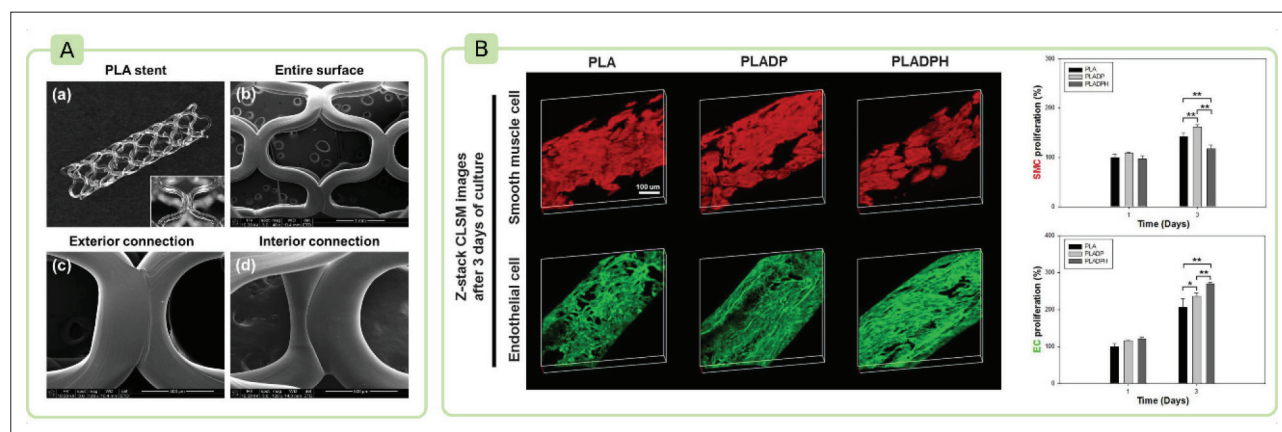


Figure 8. (A) Scanning electron microscopy of printed PLA stents: (a) full PLA stent; (b) entire surface image; (c) exterior connection; (d) interior connection. (B) Confocal laser scanning microscopy (CLSM) of smooth muscle cells (SMC, red) and endothelial cells (EC, green) seeded over the produced stents. PLA stands for pure PLA stents; PLADP stands for PLA stents after PEI immobilization; PLADPH refers to stents loaded with heparin after surface modification. Bar charts represent the percentage of cellular proliferation (both SMC and EC) at day 1 and day 3, thus demonstrating significant differences between samples. Reproduced with permission from [14] 2019, *Chemical Engineering*.

enabled the production of patient-specific polymer-carbon BRS^[70]. This study proves that patient-specific stenting process based on MEX 3DP is feasible and promising. Fibrin-directed radio-opaque contrast helps to obtain the mold and shape of the lesion, from which the 3D design of the stent is prepared. The extrusion-based printing process of the BRS was carried out as a flat rectangular slab that was subsequently folded and successfully deployed into a pig heart. Lee *et al.* have recently produced a BRS with pneumatic-based 3DP^[14]. The electronic microscopy revealed that all of the PLA strands were smooth, uniform

and clearly connected without surface damage (Figure 8A), guaranteeing absence of trauma and structural stability during implantation. To enhance biocompatibility and anti-coagulation activity, heparin was introduced through surface modification with polydopamine (PDA) and polyethyleneimine (PEI) as intermediates. This coating allows for not only a higher hydrophilicity, but also the crosslinking of heparin carboxyl groups with amino groups of PEI in the stent surface^[14]. Successful *in vivo* studies were reported, with inhibited neointima hyperplasia and absence of thrombosis. These performances can be entirely

ascribed to the presence and control release of heparin. On the other hand, the functional groups in the stent surface did influence the medical device interaction with cells and mechanical properties. The amine-rich surface of the stent with PDA and immobilized PEI promoted rapid smooth muscle cells (SMC) proliferation, while the opposite happened for the heparin-loaded stent (Figure 8B). On the other hand, heparin-loaded stent increased endothelial cells (EC) proliferation (Figure 8B) and nitric oxide generation, which is desirable for a good patency. The combination of PLA, PDA, and PEI enhanced segmental compression, bending and foreshortening tests. Even if the addition of heparin weakened the mechanical performance, it enhanced the stent flexibility^[14]. More recently, a MEX 3D printer has been used to obtain a BRS, photocurable, shape memory cyclodextrin-PCL-paclitaxel (β CD-PCL-PTX) stent, which has appropriate tensile strength, elasticity, and bursting pressure^[71].

More recently, SC-3DP has also been proposed for the production of VS medical devices. As previously emphasized, SC-3DP is considered a PBF or MEX 3DP, depending on the ingredients and the printing process. Singh *et al.* used this technique to obtain a PCL-carbonyl iron powder (CIP) stent-like structures^[72], meaning that they worked with a polymeric base dissolved in an organic solvent that evaporated as extruded. No sintering is required and debinding occurs by evaporation of the organic solvent. The authors highlighted the fact that no other previous studies have ever reported the use of this 3DP process as a VS manufacturing technique. Nevertheless, no VS 3D constructs were produced, but the attention was focused on the effect of CIP as a PCL reinforcement as well as on the final biological performance of the printed composite. The role, properties and potential usefulness of CIP will be addressed in later sections.

4.2. Vat photopolymerization 3DP as vascular stent manufacturing technique

As previously mentioned, VPP 3DP techniques work with a liquid raw material that undergoes solidification by different mechanisms, depending on both the material itself and the specific 3DP methodology used. For the production of VS, photocrosslinkable resins and polyesters are able to provide suitable mechanical properties after curing; therefore, they can be used as vascular endoprosthesis.

Micro-continuous liquid interface printing (micro CLIP) is a technique that works with a similar principle to that of DLP. The speed, reproducibility, and fidelity of this 3DP possess a high potential in the production of in situ, tailor-made BRS. Van Lith *et al.* used a customized micro CLIP for the production of a photocurable, antioxidant and bioresorbable metacrylated biomaterial (poly(1,12-

dodecamethylene citrate), mPDC) by mixing citric acid and 1,12-dodecanediol, THF^[73]. The photocuring process transforms the initial material into a bioresorbable one, which can be used as a biomaterial ink for the production of VS and shows *in vitro* degradation of 25% (PBS, 37°C) within 6 months. Upon deployment, the fabricated stent was able to self-expand properly, reaching the original diameter in just 3 min. This self-expansion was reported to be faster than the expansion of other commercial BRS, taking time from 3 to 8 min. Moreover, the final mechanical properties of these 3D-printed BRS were comparable to bare-metal nitinol stents, making them a feasible formulation for the production of customizable, personalized BRS. Later, authors reported an in-process calibration method for the same micro CLIP printing process, aiming to reduce the total fabrication time from 70 min to 20-11 min depending on the layer slicing thickness of the stent^[74]. They also optimized the ingredients and concentrations during the printing process by including two photoinitiators: irgacure and ethyl 4-dimethylamino benzoate (EDAB). This combination enabled greater crosslinking and made possible strut geometries.

Photocrosslinkable, elastomeric polyesters such as metacrylated poly(dodecanediol citrate) (mPDC) can be used as raw materials for the production of 3D constructs by means of DLP. mPDC polymer has proven to be biodegradable and biocompatible and possess elastic behavior, making it suitable for the production of self-expandable BRS^[75,76]. Oliveira *et al.* developed a BRS, DES based on mPDC and nitric oxide, and used DLP as 3DP technology to produce a small diameter VS (Figure 9A)^[75]. With respect to other active substances, nitric oxide has proven to be more advantageous for stents in terms of cellular proliferation, biocompatibility and restenosis. Moreover, nitric oxide is beneficial to maintain the muscular tonus of the vasculature under treatment, control blood pressure and inhibit platelet adhesion. Although the authors proposed this approach for a coronary stent, its translation into a peripheral one could be more beneficial if blood pressure and muscle tone of the peripheral vessels are lower with respect to coronary arteries. Moreover, it has recently been demonstrated that the nitric oxide system and its regulators are compromised in PAD^[77]. Nitric oxide release was achieved by the S-nitrosation of N-acetyl-d-penicillamine (SNAP) of the 3D-printed construct via liquid adsorption^[75]. The self-expanding properties of the stent were confirmed due to good elastic response up to 50% strain. In fact, the stent completely recovered its initial dimensions after being collapsed and crimped (Figure 9C). Nevertheless, the authors stated that an optimal cure is needed for the mechanical properties to be maximized, meaning that the DLP printing process

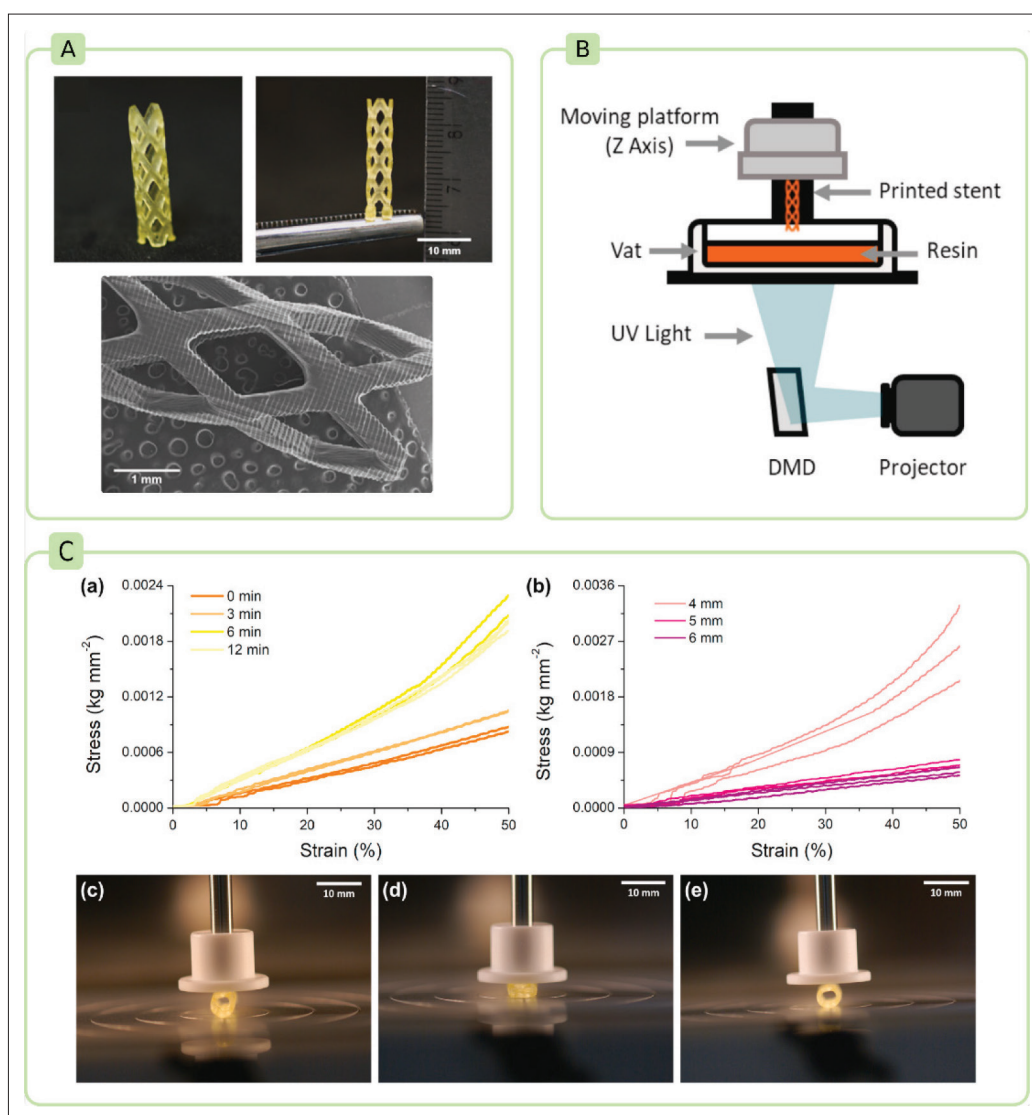


Figure 9. (A) Photographs and scanning electron microscopy of mPDC-SNAP stent. (B) Schematic representation of the DLP printer used. (C) Stress-strain compression curves for uncured and post-cured mPDC stents at different times and with different diameters (a and b). Photographs frames of a stent of 6 mm diameter during stress-strain compression test (c–e). Reproduced with permission from [75] 2021, *Bioprinting*.

(Figure 9B) must be previously optimized. The release of nitric oxide from mPDC/SNAP BRS is directly related to the surface in contact with the aqueous biological medium, suggesting that the modulation of the final stent geometry can be an important variable to control the nitric oxide release^[75]. This can be interpreted as follows: 3DP enables the production of customized VS in terms of not only dimensions, but also particular therapeutic needs when it comes to DES.

4.3. Material jetting 3DP as vascular stent manufacturing technique

MJT 3DP is based on the deposition of liquid droplets. It is complicated to obtain intricate, high-resolution structures

such as those required for the production of VS by this 3DP technique. Moreover, the manufacturing of MJT-printed constructs depends on the rapid solidification or instantaneous curing (such as photo-crosslinking) of the droplets as they are deposited, in an attempt to minimize the liquid ink to flow over the previously deposited layer. Under these circumstances, MJT is a challenging technique when it comes to VS. Nonetheless, it can be of great usefulness in combination with other methods.

In an attempt to improve the drug coating process of stent struts, Scutaris *et al.* referred MJT 3DP to as a reliable, robust, and reproducible technique in controlling and guaranteeing the proper drug-coating of an intravascular

stent^[19]. The quality of stent drug-coating is crucial for two main reasons: (i) it influences the drug release rate, and (ii) it affects the superficial texture of the VS as an irregular coating could lead to rough surfaces. Therefore, a smooth stent surface would minimize the injury of blood vessels during the implantation of the medical device. They aimed to improve the traditional stent drug-coating procedures, thereby reducing the time required and material waste. Thus, they MJT-printed PLA/simvastatin and PLA/paclitaxel solutions over different already-existing BMS (PresillionTM and CypherTM stents) by means of a piezodriven dispenser. The authors reported that “tips with 300 pL aqueous droplet volume are suitable for stent coating (...) while smaller volumes (100 pL) resulted in clogging of the nozzle”^[19]. Another important factor to bear in mind is the voltage used, since an inadequate voltage could lead to bubble formation inside the ink tip, jeopardizing the printability. The comparison between the final coating of two commercial stents with different geometries indicates the need for MJT drug-coating optimization according to the shape of each medical device to avoid irregular drug-coating. The *in vitro* drug release profiles of simvastatin and paclitaxel, separately, revealed burst release for the first 5 days, followed by a first-order release until day 30 in both cases. A successful implantation in male Wistar rats was reported, without inflammatory and cytotoxicity response within 7 days. Therefore, MJT-printing for stent drug-coating can be used to optimize and maximize the performance of DES.

4.4. Powder bed fusion 3DP as vascular stent manufacturing technique

PBF 3DP is usually associated to strong, hard materials. In fact, metal powders are most frequently used in PBF 3DP techniques to obtain metallic VS. Despite the long-term complications and disadvantages of permanent metallic stents, they are the most widely used (Table 1, Figure 2). Nevertheless, in terms of cutting-edge technologies and research, the efforts are centered on BRS, DES, which means that the number of studies dealing with PBF 3DP techniques is scarce.

Laser-cutting and braiding are the most commonly used manufacturing techniques for the production of metallic VS. When it comes to 3DP, PBF is commonly used to print metallic materials. Demir and Previtali demonstrated the feasibility and convenience of PBF and the subsequent electrochemical polishing to produce a CoCr stent with respect to the conventional manufacturing cycles (microtube production followed by laser-cutting)^[37]. In this technique, different scan strategies can be followed (parallel or concentric scanning), giving rise to different results. The authors highlighted the importance of a proper

stent design and manufacturing orientation together with some basic rules during PBF printing process. With PBF printing, layer plane supports are needed when angles smaller than 45° are created; overhanging regions up to 1 mm can be built without supports; minimum gaps of 0.3 mm are recommended between separate features, etc.^[37] According to these requirements, they designed a stent with hexagonal, zig-zag pattern forming a closed cell without flex-connectors (Figure 10A). This geometry avoided the requirements of support structures during PBF 3DP. Their attention was clearly centered on the optimization of the 3DP manufacturing, not in the final properties of the final stent, so the tensile strength, recoil and fatigue resistance were not characterized in this study. Depending on the laser scanning pattern, the laser pulse duration and peak power must be optimized. They also concluded that increased peak power and pulse duration reduced surface roughness. For the particular geometrical design of this VS, the parallel strategy gave rise to irregular geometry, thickness, and surface roughness, thus highlighting the inadequacy of this strategy for the production of micro-geometries (Figure 10C). On the contrary, concentric scanning and higher printability were achieved (Figure 10C). Additionally, PBF 3DP produces items with very rough surfaces, implying that post-processing techniques such electro-polishing are compulsory to reduce harm during stent implantation (Figure 10B)^[37].

Despite the fact that metallic substrates are the most frequent in PBF, there are also some exceptions. For instance, some years ago, Flege *et al.* adapted the PBF 3DP technique to produce a BRS vascular stent made of PLLA and PCL^[78]. Since this 3DP technique requires powdery raw materials for the printing process, PLLA and PCL polymers were subjected to solvent-evaporation processes to obtain homogeneous, small particles so that they could then be used in PBF; both PCL and PLLA particles possessed good flowability, regular spherical shape, narrow particle size distribution, and high density. Moreover, the laser of the PBF printer was adapted by adding a power attenuator. The attention of this study was therefore centered on the ability to produce stents from these raw materials and to monitor the stability of the resultant ingredients after the PBF printing and gamma-irradiation sterilization. The biocompatibility of the stents and the materials was assessed using human arterial smooth muscle cells (haSMCs), human umbilical vein endothelial cells (HUVECs), and endothelial progenitor cells (EPCs). First, the manufacturing of PCL and PLLA powder particles did not jeopardize their biocompatibility, unlike the printing process, which reduced metabolic activity of the EPCs. The authors ascribed this result to the presence of polymerization initiators in stent

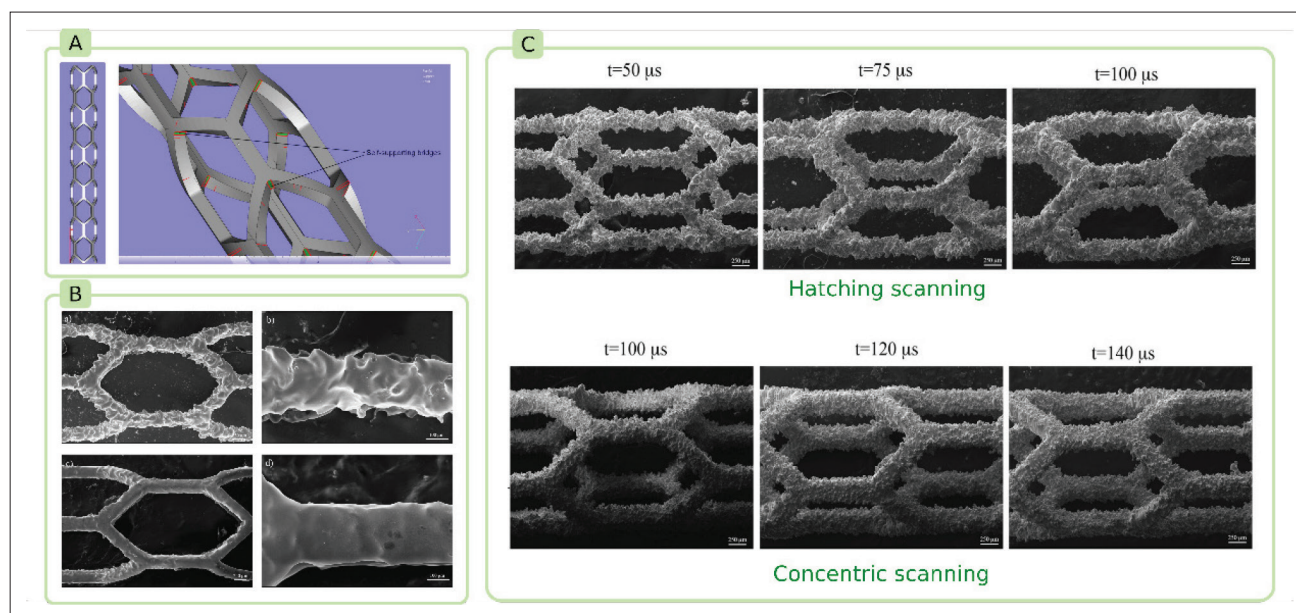


Figure 10. (A) Digital stent prototype optimized for PBF 3DP. (B) Scanning electron microscopy images of printed VS after electrochemical polishing; images at the upper panel belong to VS produced by hatching PBF scanning, whereas images at the lower panel correspond to a stent produced with concentric scanning PBF. (C) Scanning electron microscopy images of 3DP CoCr VS produced by hatching (top) or concentric strategy laser scanning (bottom) and their differences. Laser pulse duration is indicated in each case. Reproduced with permission from [37] 2019, *Materials & Design*.

surfaces. Gamma-irradiation was an effective sterilization procedure, although it also affected the structure of the polymers and their biological performance. haSMCs proliferation and metabolic activity were inhibited due to surface modifications of the polymers during sterilization, while EPCs were unaffected. Flege *et al.* highlighted this result as a positive one, since it “might favor the prevention of neointimal hyperplasia in stented vessels”^[78]. This study demonstrated the versatility of 3DP techniques to be adapted to print a wide variety of materials, meaning that none of them can be dismissed as useful ally in the production of medical devices in future.

5. Computational studies and 3D printing

Several studies have demonstrated that stent design features are of great importance for a successful treatment due to correlations with thrombosis and in-restenosis risk^[33,79,80]. For better clarity and understanding of this section, a schematic representation of the most important stent parts and their nomenclature are included in Figure 11A.

The implanted VS induces disturbances in blood flow and alters shear stress of wall vessels at the strut level. These factors highly influence the pathophysiological mechanisms leading to VS complications^[81]. Focusing on the structural and geometrical design of VS, the first manufactured stents could be classified into slotted geometries and coil geometries. The former ones possessed

higher radial strength but lacked flexibility, as compared to their coil counterparts. Afterward, VS geometries have greatly evolved and changed, with more complicated and perfected geometries included, and are adapted to their final scope (Table 3). Nowadays, coil stent geometries are more commonly used for non-vascular stents, being more frequent to find helical spiral designs for VS. Woven (braided or knitted) designs can be made of more than one strand (made of different materials) and they are traditionally used for the production of self-expandable VS, although balloon-expandable examples can also be found. VS with individual rings frequently use zig-zag wire (struts) that should be attached to one another to form the final stent or vascular prosthesis. If individual rings are connected to each other with a certain consistent pattern, the stent possesses the so-called “sequential ring connection.” In this occasion, the zig-zag struts are connected through “bridges,” “hinges,” or “nodes,” placed in every strut inflection point (regular connection), in a subset of inflection points alternating with unconnected ones (periodic connection) or they can be placed to join the outer radii (peak-peak bridging elements) or to join inner radii with outer radii (peak-valley bridging elements). The stent bridges can have different shapes such as V, L, N, W, S shapes, etc., as well as multiple shapes all combined in the same structure (Figure 11C). These connections play an important role in the optimization of the final performance of the stent, especially in their

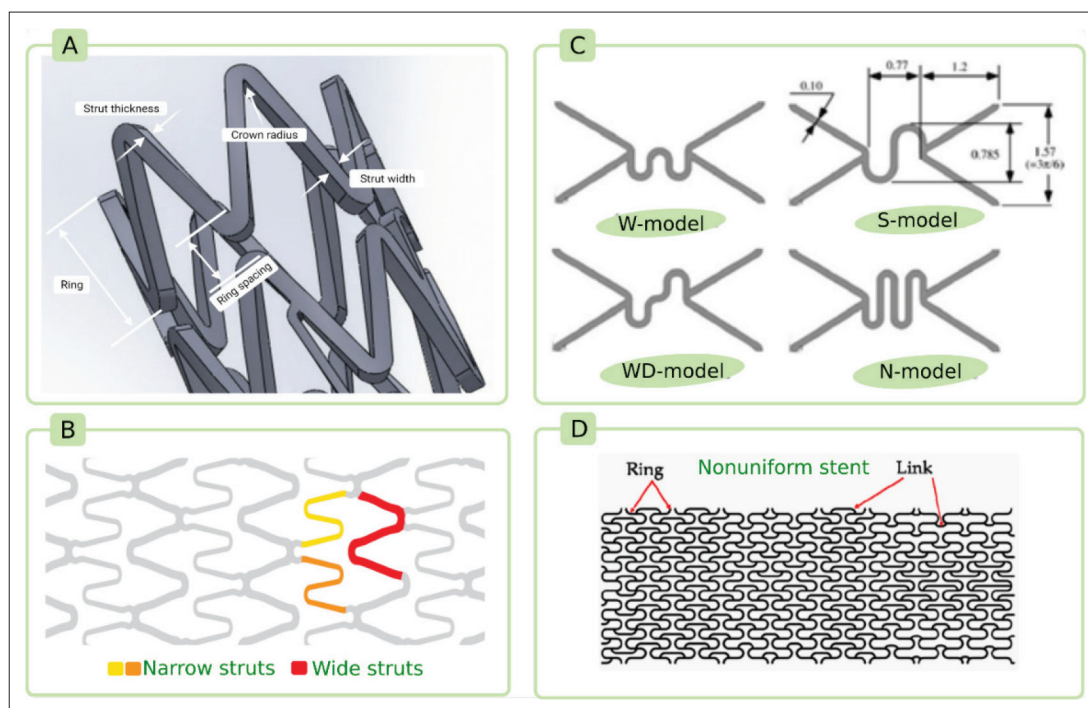


Figure 11. (A) Schematic representation of stent parts and nomenclature. (B) Geometrical design of commercial NIRxcell stent, which possesses different strut widths within the same structure. (C) Some examples of strut connections. (D) Non-uniform Poisson's ratio stent 2D structure. Reproduced with permission from [82] 2021, *Micromachines*.

mechanical properties, as recently reviewed by Pan *et al.*^[82] Within these stents, it is possible to differentiate between “closed cells” and “open cells” (Table 3)^[28]. Nowadays, it is also possible to find commercial stents with different strut width in the same device, such as NIRxcell™ stent system (Figure 11B) and others with non-uniform cell sizes and shapes (Figure 11D).

The preparation of different stent designs and the experimental study of their correlation with stent performance and future complications is not feasible from an experimental point of view due to the milieu of possible designs (Table 3), dimensions, materials, hemodynamics, etc., together with the long-term studies and the number of replicates. For example, some authors and manufacturers advocate for stents with thinner struts to improve and aid re-endothelialization^[83,84], but this can significantly influence the VS deliverability, flexibility, friction, amount of vessel wall coverage, and drug delivery, if applicable. In this regard, computational studies or *in silico* studies are of great usefulness, enabling digital simulations to predict the final properties and performance of a particular stent. From a medical point of view, 3DP is an especially robust, versatile technique for the manufacturing of personalized, *in situ* VS prior to the surgical intervention and adapted to the particular type of lesion and blood vessel. From the research point

of view, 3DP is also useful in the production of stents with different geometries enabling the study of the influence that each design would be upgraded to as a medical device. Therefore, 3DP is the perfect method for rapidly confirming or denying computational studies.

Misra *et al.* used computational studies to explore different PCL-GR geometries and simulate the deformation of the stent during crimping and expansion^[70]. The simulations helped to discern the most optimal stent design, thus accelerating the production of the CAD model for 3DP. In a similar way, Cabrera *et al.* used computational studies to translate the results into a physical polymer prototype through FDM 3DP^[85]. The idea was to fabricate a stent with a flexible, BRS thermoplastic co-polyester elastomer (TPC) having physical properties similar to that of a commercially available nitinol stent, including self-expanding ability. Computational studies enabled the anticipation and adjustment of the final stent performance by changing the width, thickness, and strut number. After selecting the desirable stent parameters, dimensions and geometry as well as obtaining adequate crimping and crush computational results, the TPC stent was printed with FDM. The experimental mechanical studies were in agreement with the computational models, confirming the ability of computational simulations to build realistic prototypes.

Table 3. Classification and features of most frequently used VS designs and geometries


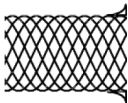

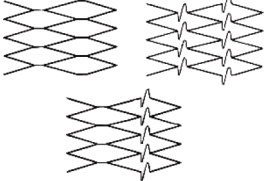
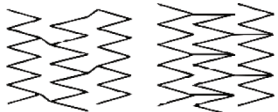
Geometry	Scheme	Strengths	Weaknesses
Helical spiral		<ul style="list-style-type: none"> • High flexibility (minimal internal connection points) • Can be subjected to elongation and compression during delivery 	<ul style="list-style-type: none"> • Lack of longitudinal support
Woven (braided, knitted)		<ul style="list-style-type: none"> • Offer remarkable coverage of the stenosed region 	<ul style="list-style-type: none"> • Frequent recoil events after expansion • Radial strength dependent on axial fixation of their ends
Individual rings		<ul style="list-style-type: none"> • Useful as vascular grafts • Easy to produce • Highly flexible • Versatile 	<ul style="list-style-type: none"> • Require additional support or connection with other pieces/rings
Sequential rings	Closed cells (peak-to-peak connections) 	<ul style="list-style-type: none"> • Regular bridging elements lead to improved strength • Optimal scaffolding and support • Flex connectors (with different shapes) allow for higher flexibility due to plastic deformation of the bridging element during implantation 	<ul style="list-style-type: none"> • Generally less flexible than opened structures, especially if too much bridging, rigid connections are used
	Open cells (peak-to-peak, peak-to-valley, myriad of hybrid combinations). 	<ul style="list-style-type: none"> • Longitudinal flexibility thanks to unconnected struts regions • Peak-to-valley connections optimize scaffolding due to higher alignment 	<ul style="list-style-type: none"> • Peak-to-valley sacrifices strength with respect to peak-to-peak connections

Table constructed based on the review of Stoeckel *et al.*^[28].

6. The importance of ingredients for the manufacturing of vascular stents

In the development of cardiovascular grafts and stents, the use of material such as nanocomposites has greatly evolved throughout the years. A nanocomposite is a material of heterogeneous composition (organic, inorganic or hybrids) including ingredients mixed at the nanometer scale. Usually, nanocomposites are made of a polymeric-like matrix hosting another ingredient with functional activity (therapeutic, crosslinking, reinforcing, etc.). Apart from the composition and ingredient concentration, the production methodology is also important for the successful nanocomposite performance, including production technique, type of ingredients, reactions/interactions between the nanocomposite components, among others^[86]. Clays, carbon, metals and glass ingredients have proven their usefulness as nanocomposite reinforcing or fillers, enabling not only the carriage and delivery of therapeutic ingredients, but also the improvement of mechanical features and rheology. When it comes to medical devices,

the biocompatibility of the nanocomposite is crucial to guarantee their safety after implantation.

In the particular case of cardiovascular medical devices (vascular grafts and VS), carbon-based ingredients (carbon nanotubes, graphene, etc.) have proven their biocompatibility^[86]. Graphite, graphene, and carbon nanotubes are allotropic carbon forms, which differ from each other by spatial disposition. Graphene is a monolayer of carbon atoms linked to each other forming a hexagonal honeycomb lattice. Graphite, on the other hand, occurs when graphene layers are stacked in the *z*-plane and held together by van der Waals forces. Carbon nanotubes (CNT) are tubular graphene sheets. Depending on the number of tubular sheets, CNT can be divided into single-walled CNT (typically abbreviated as SWCNT) or multi-walled CNT, which is when more than two layers are combined (MWCNT). The main interest of these synthetic materials lies in their biocompatibility. Vellayappan *et al.* reviewed the usefulness of these materials in the development of vascular grafts and stents^[86]. Carbon-based materials are useful as anticoagulant ingredients and can promote cellular growth

and mechanical properties of polymers such as a PLGA, PCL, PCLA (poly(L-lactide-co- ϵ -caprolactone))^[87-92]. For the particular case of mechanical reinforcement, the homogeneous dispersion of carbon nanotubes is crucial to ascertain optimal mechanical strength^[92]. Consequently, there is no direct relationship between the amount of CNT and the mechanical improvement, since very high concentration could lead to heterogeneous dispersion, which hinders the mechanical performance of the nanocomposite.

Graphene (GR) has demonstrated to be a useful ingredient to improve both mechanical properties of VS and control drug release from drug-eluting VS. The literature regarding 3DP and GR is currently scarce, but there are clear indications of the usefulness of graphene as an ingredient to improve the mechanical and biological properties of stents. Carbon is one of the materials with higher hemocompatibility due to chemical inertness, minimal platelet activation and favorable conformational changes^[93]. Coating is the most common strategy to add GR to VS^[94-96]. Nitinol VS coated with GR had improved biological properties compared to its counterpart^[94]. Briefly, GR coating inhibited platelet activation and was fully biocompatible with smooth muscle cells. Likewise, excellent bio- and hemocompatibility was reported for a coated stainless steel VS^[96]. In this occasion, a coating mixture containing poly(3,4-ethylenedioxythiophene) polystyrene sulfonate (PEDOT:PSS), graphene oxide (GO), and heparin was deposited over the stainless steel VS (SUS316) by electrochemical polymerization. This process gave rise to a stent with high hydrophilic nature, which can prevent platelet adhesion following implantation. GO contributed the most to this effect, while the role of heparin was the minimum. The authors hypothesized that the negative charge of GO created a repulsing force against plasma proteins and platelets (also with a negative net charge)^[96]. On the opposite side, GR has also been shown to be a useful coating in BRS stents. Magnesium alloy stents are BRS VS with good mechanical properties. Nonetheless, these stents suffers from a rapid degradation and insufficient biocompatibility. Layer-by-layer deposition method was recently used to coat magnesium alloy VS with GR functionalized with chitosan^[95]. The authors stated that the resultant bioactive multilayer coating endowed magnesium alloy with excellent *in vitro* degradation resistance. Additionally, good blood compatibility (reduced hemolysis and platelet adhesion) and improved expression of vascular endothelial growth factor (VEGF) and nitric oxide were ascribed to the GR-based coating.

The study of Misra *et al.* is one of the few dealing with 3DP, graphene, and VS^[70]. A BRS stent made of

PCL and graphene and loaded with niclosamide and inositol phosphate reported good anticoagulation and antirestenosis performance. The comparison of the 3D-printed stent with and without graphene helps discern the influence of the inorganic ingredient on the stent performance. The presence of 4% of graphene increased the Young's modulus of PCL and demonstrated better resistance under artery wall pressure after deployment. By the same token, PCL-graphene stent had a better control of niclosamide and inositol phosphate release.

One of the limitations of 3DP for the production of VS lies in the fact that most of the materials used are polymeric, but not all of them are able to be deployed inside the vessels. In this regard, shape memory polymers (SMP), also known as "smart" or "intelligent materials" are currently on the spotlight, not only for 3DP in general^[97], but also in the production of VS. In fact, smart materials such as shape memory alloys (such as nitinol) have already been used to fabricate VS, and most of them have been commercialized. SMP are polymeric smart materials with the ability to change their shape while subjected to some triggers such as temperature, electromagnetic fields, photo-activation, electro-activation, contact with water (swelling), pH medium changes, etc. Disregarding the triggering stimulus, all these smart materials are used in a two-step manner^[97,98]. The "programming step" is the shape-memory creation process, where the permanent, original shape is changed to a secondary (temporary) one by subjecting the material to external stress forces (mechanical stress). Under these circumstances, the SMP acquires a desirable shape and maintains it after stress removal. Then, after the exposure of the shaped structure to other non-mechanical triggers (e.g., heat, light, pH change), it is able to recover the original, permanent shape by reverting the shape it acquires during the application of mechanical forces. Hence, SMP have the ability to store mechanical stress and release it under non-mechanical stimuli. Depending on the nature of the material, the mechanism of shape modification is different. For the particular case of SMP, they share the presence of "permanent netpoints" or "permanent links" in their internal network structure and "temporary links" or "switches." The permanent links are responsible for the permanent shape, the so-called "memory effect," and therefore, these netpoints are not affected by mechanical deformation. On the other hand, switches are formed during mechanical stress due to the conformational freedom of some of the polymer chains. The deformation obtained during the programming step can be stabilized by the formation of these "temporary links" within the polymer structure. When it comes to thermal-sensitive polymers, the difference between permanent links and temporary links lies in the existence of more than

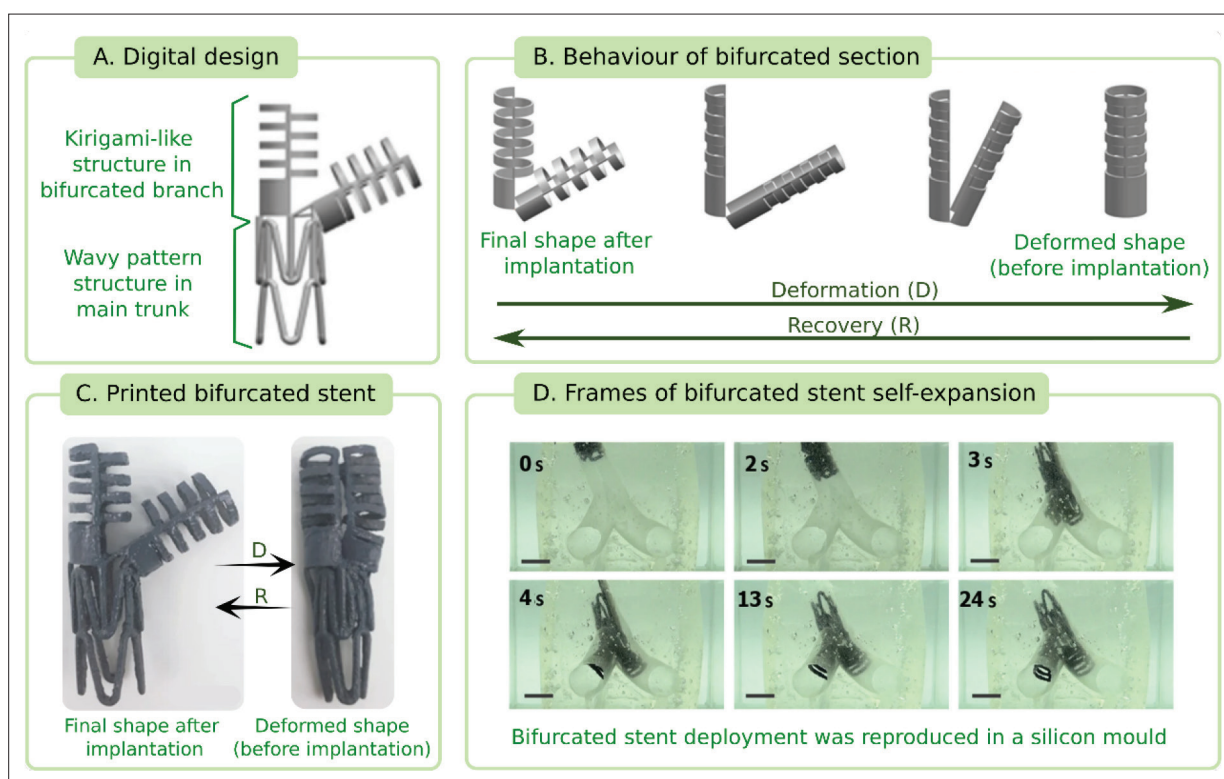


Figure 12. Design and real aspect of bifurcated self-expandable stent produced by FMD using a shape memory polymer. The bifurcated branch is able to deform until the formation of a single conduit, thereby allowing implantation. The suitability of this VS for deployment in a bifurcated vessel was tested in a silicon, transparent mold. Scale bars: 20 mm. Reproduced with permission from [66] 2018, *Scientific Reports*.

one thermal transition. Those domains with the highest thermal transition (glass transition temperature, T_g or melting temperature, T_m) are responsible for the memory shape or permanent shape, whereas switching domains that possess the second highest thermal transition (T_g or T_m) is responsible for the temporary shape^[97,98]. SMP also possesses useful properties, such as lightweight, large elastic modulus and flexibility, as well as biodegradability^[97].

A polyurethane SMP was successfully used to obtain a bifurcated stent deployable in just one step^[65,66]. When vascular stenosis occurs in a bifurcated vessel (vessel with Y-shaped lumen), two cylindrical stents must be inserted and subsequently joined, which complicates the intervention. Thanks to the intrinsic properties of SMP, Kim *et al.* were able to fabricate a one-piece, bifurcated stent combining two different geometrical designs: the trunk of the stent (main vessel) possessed a conventional wavy pattern, whereas the bifurcated zone was designed with a “kirigami-like” structure (Figure 12A). Kirigami is a superset of origami with the addition of cutting^[66]. For deployment, an intelligent strategy was also applied: the two bifurcated vessels will be folded and fitted with one another (like a puzzle) to form a full, cylindrical piece that will be taken to the deployment area (Figure 12B). Once

there, the folded branches will bifurcate and deployed in both vessels in just one step after the application of temperature as a trigger (Figure 12C)^[65,66]. The main drawback of this particular stent was the mismatch between the temperature that triggers the SMP to unfold (55°C – 60°C) and the temperature of the human body. A recent study demonstrates the possibility of modifying the glass transition temperature of SMP, bringing it closer to a more physiological temperature range^[64]. The authors synthesized biodegradable poly(glycerol dodecanoate (PGD, transition temperature of 22.5°C – 43.6°C) and subsequently modified it to obtain poly(glycerol dodecanoate acrylate) (PGDA) through glycerol and docecenedioic polycondensation. The resultant material was photocurable and showed a final transition temperature of 20°C – 37°C , which was much closer to the physiological range. After being printed and photocured with UV light, the PGDA construct was thermally cured at 145°C in an oven. Then, the construct was deformed to create the “crimped state” of the stent. With further heating above the transition temperature (20°C – 37°C), the stent recovered its initial state within 8 seconds. Similar mechanical properties between the printed stent and the soft biological tissues at 37°C was found, demonstrating mechanical adaptation

of the printed construct after biomedical implantation^[64]. PLA is a SMP with non-irritant, biocompatibility and biodegradability features. This material, in combination with PVA and FDM 3DP, has proven to be useful in the production of stents with feasible mechanical properties and minimal invasive implantation^[62]. PLA proved to be a promising material for self-expandable stents, with a diameter recovery ratio above 95% and length recovery ratio above 97%. One of the disadvantages of the system lies in the glass transition temperature of PLA (50-80°C), which is 13-43°C above the human body temperature, thus complicating the implantation procedure. Further studies regarding material properties and modification are needed to prove PLA as a stent material.

Sulfated chitosan was used to modify the surface of the PCL-printed stent by immobilization of 2-N, 6-O-sulfated chitosan, which gives rise to a so-called "aminated stent"^[36]. The amination of PCL affected the surface microstructure and the resultant interaction of the stent with cells after implantation. In fact, despite that both modified and unmodified PCL stents possessed adequate biocompatibility, the cellular proliferation was enhanced after the surface modification. This result has been explained by the roughness of the surface: "rough surface of stents can highly improve endothelial cell attachment and growth, while smooth surface contributes to endothelial cell migration"^[36]. According to scanning electron microscopy images, the addition of sulfated chitosan improved the superficial roughness, in agreement with the biocompatibility and cellular proliferation results. The surface modification did not influence the mechanical properties, which is expectable since the amination is performed after the 3DP process.

Among the SMP, PCL is one of the most currently studied for 3DP of VS due to its high mechanical properties and tunable transition temperature. PCL has been recently modified by the addition of cyclodextrin and acrylation^[71]. The acrylation enables the photopolymerization of the final 3D construct and further improves the final consistence and mechanical properties. The lyophilic nature of both PTX and PCL implies their combination to be feasible and homogeneous. Nonetheless, an excessive hydrophobicity of the final system jeopardizes the biocompatibility of the stent as well as the release and dissolution of PTX. The presence of β -cyclodextrin (β CD) aims to improve the hydrophilicity of the resultant stent, therefore compensating the hydrophobic nature of PCL. CDs are well known by their role as drug solubilizing agent. PTX can bind well to the inner cavity of β CD to form easily soluble inclusion bodies. Sustained release of PTX was reported for 15–20 days, revealing higher performance with respect to other similar, commercially

available stents. After implantation, the β CD-PCL-PTX stent recovers its shape at 56.8°C, which can be achieved with a balloon containing hot water^[71].

Carbonyl iron powder (CIP) is a pure form of iron used in a wide variety of applications, from dietary supplement to inductive electronic components. In our particular case, CIP has proven to be very useful for the reinforcement of polymers thanks to its high physical strength^[99]. Together with the biocompatibility, antithrombotic effect and negligible toxicity of CIP^[100-103], CIP is an ingredient with remarkable potential in the formulation of vascular prosthesis such as VS. CIP has been combined with PCL in an attempt to improve the properties of the polymer^[72]. The combination PCL-CIP was purely based on physical interactions (no chemical interactions were detected). The addition of 2% CIP improved the mechanical performance of PCL structures, including its flexibility. Moreover, the hydrophobicity of PCL was reduced by the presence of CIP, with hydrophilic profile. This amount of CIP demonstrated *in vitro* that the PCL-CIP composite is adequate as stent ingredient. The structures were biocompatible, hemocompatible and non-thrombogenic. An indirect correlation between the concentration of CIP and the activation of platelets was reported (the higher the amount of CIP, the lower the platelet activation)^[72].

Shape memory alloys (SMA) can also be 3D-printed by using PBF techniques. Different studies have revealed that the use of 3DP (such as PBD or DED) for the production of nitinol 3D structures (not specifically VS) is very promising but requires the optimization of several parameters^[104-107]. No major studies have been devoted to the specific manufacturing of nitinol VS through 3DP. The study of Lei *et al.* (2020)^[68] reported the use of nitinol as part of a personalized VS, but 3DP was solely used for the fabrication of an aortic mold where nitinol wires were subsequently placed (Figure 7).

Table 4 gathers the most recent studies on the production of VS by 3DP methods and their main features. It is clear that bioresorbable vascular stents (BRS) are currently in the spotlight due to their advantageous properties with respect to permanent stents. The vast majority of materials recently used are synthetic polymers, which are more versatile and apt for 3DP techniques such as DED (FDM) and MEX, both of them are considered the most cost-effective 3DP techniques^[108,109]. Moreover, polymers are in general pliable, they can be fabricated with different mechanical properties, and some of them are biodegradable and biocompatible. Additionally, shape-memory polymers are of great usefulness for the production of self-expandable devices. In fact, PCL is the most frequently used materials, followed by PLA, in the printing of VS (Table 4) due to its biodegradability, biocompatibility, and shape memory

Table 4. Compilation of the VS most recently produced by 3DP and their main features

Type of stent	Implant methodology	Material	3DP technique	Drug-eluting stent	Blood vessel type	Ref.
BRS	Not specified	PCL, PLGA, PEG	MEX (rotatory mandrel as printbed)	Sirolimus	Coronary	[69]
BRS	Self-expandable	mPDC	Micro-continuous liquid interface printing (DLP)	-	Coronary	[73]
BRS	Not specified	PCL, PLA	FDM (rotatory mandrel as printbed)	-	Coronary	[59-61]
BRS	Self-expandable	TPC	FDM	-	Not specified	[85]
BRS	Self-expandable	PCL, GR	MEX	Niclosamide, inositol phosphate	Coronary	[70]
BRS	Self-expandable	PLA	FDM	-	Coronary	[63]
BRS	Self-expandable	PLA	FDM	-	Coronary	[62]
BRS	Balloon-expanded	PLLA	FDM (rotatory mandrel as printbed)	Sirolimus	Coronary	[67]
BRS	Balloon-expanded	PLA, PDA and PEI coating	MEX	Heparin	Coronary	[14]
BRS	Not specified	PCL	FDM (rotatory mandrel with voltage as print-bed).	-	Coronary	[36]
BRS	Self-expandable	PCL, β CD	MEX (rotatory mandrel as printbed)	Paclitaxel	Peripheral	[71]
BRS	Self-expandable	PGDA	FDM	-	Not specified	[64]
BRS	Self-expandable	mPDC, SNAP	DLP	Nitric oxide	Coronary	[75]
BMS (Presillion™ and Cypher stents)	Balloon-expanded	PLA/drug as stent coating	MJT (inkjet printing)	Simvastatin, paclitaxel	Coronary	[19]
Not specified	Self-expandable	SMP (not specified)	FDM	-	Not specified	[65],[66]
BMS	Not specified	Nitinol-PU	FDM (used for the creation of a sacrificial core)	-	Not specified	[68]
BMS	Not specified	CoCr	PBF	-	Coronary	[37]

The table is mainly sorted by type of stent.

properties. Because of the intrinsic degradation of BRS, they can easily act as DES, controlling the release of actives as they degrade, a feature that is also possible to obtain when polymers are used.

7. Future directions

This section provides an overview about the potential strategies to follow in the endovascular prosthesis field.

The combination of different manufacturing techniques is one of the approaches most commonly used to improve VS^[19,36]. For instance, the involvement of one or more 3DP strategies in this process could potentially enhance VS industry, allowing for a better control of not only the mechanical performance of medical device, but also their biodegradability or the controlled drug release.

It is undeniable that PAD lesions are much more complicated to treat due to the particularities of the disease itself as it is associated with wider lesions (sometimes in branched blood vessels) located in vessels distant from the heart. This entails lower blood pressure and oxygenation, which complicates not only the intervention, but also the prognosis in comparison with CAD lesions. In view of these facts coupled with their economic burden, it is imperative to make some progress in the design and production of specific VS to address lesions in peripheral vessels (peripheral VS). Even modest progresses in this direction will be a significant step forward to improve PAD treatment and prognosis.

Regarding the mechanical properties of a VS, there are still some unresolved issues. The greater the radial stiffness of the VS, the higher the pressure on the vascular wall and

the better the vascular flow. On the other hand, a greater axial flexibility would bring about better adaptation of the VS to folding or deformation and to natural curvature of the native vessel, thus reducing the damage to the vascular wall. Finding a compromise between these two contradictory but coexisting features (axial flexibility versus radial rigidity) is one of the main challenges in the contemporary design of stents. On top of that, it could also be useful to fabricate stents with different mechanical properties along the structure. Both ends of the VS are the most conflicting area in hyperplasia, since the damage over the vessel is higher in these zones. It could be feasible using 3DP and a mixture of different materials.

The materials and their concentration are crucial for the mechanical properties of the VS, and their structural design also plays an important role. In this regard, 3DP and computational studies could mark a milestone since they enable the study of several structural designs at the same time (computational studies) and their rapid reproduction (3DP) to confirm or deny the predictions made with calculations, not to mention the possibility of adapting the designs to a particular artery, material or type of lesion. The idea of some researchers to combine both strategies^[70,85] is promising and can be envisaged as an intelligent approach for future directions in the research and development of VS.

Ingredients such as graphene or CNT, together with CIP, have been recently proposed for the development of VS through 3DP^[70,99]. The use of these ingredients has been mostly motivated by their already demonstrated ability to reinforce materials such as polymers, together with their role as drug carriers that are able to control drug release, which also make them good candidates for the production of DES. Apart from graphene and CNT, similar inorganic ingredients such as natural and synthetic clay minerals (e.g., montmorillonite, laponite, and layered double hydroxides [LDH]) also have a lot of potential in the present matter, acting as mechanical reinforcement^[110-115] and drug delivery systems^[116-118]. The vast majority of DES are loaded with antithrombotic, antiproliferative, immunosuppressive, or anti-inflammatory drugs. Nevertheless, for disorders such as PAD, the use of nitric oxide as an active ingredient seems a reasonable candidate. In this regard, LDHs and other inorganic ingredients such as zeolites can act as a persistent and stable reaction mediator (catalyst) for the production of nitric oxide for inhalation therapy^[119-121]. This ability of LDH and zeolites as carriers and catalysts of nitric oxide could be potentially applied for the design of peripheral VS in the future.

As far as we are concerned, the use of the aforementioned ingredients (montmorillonite, laponite, LDH) for the development of VS is currently scarce, probably because of

their undefined hemocompatibility and biodegradability. When it comes to hemocompatibility, LDHs apparently show a better performance than other clay minerals^[122-129]. Nevertheless, it is also well-known that these materials can be modified or functionalized by their combination with chemical ingredients to adjust their final properties and performance^[130-132]. The surface functionalization or organomodification or inorganic ingredients would enable the adjustment of their final properties and the reduction of undesirable effects that may occur. A LDH has been recently used as an ingredient of a biodegradable coating intended to be used in a DES^[133]. The final aim of this coating was to minimize neointimal hyperplasia associated with BMS. The drug-eluting coating consists of a PLA-PEG-heparin copolymer loaded with LDH-biochanin-A composite. Biochanin A is an isoflavone phytoestrogen with antiproliferative and vasculoprotective properties. In this particular case, LDH not only acted as carrier and controlled release agent, but also as a protective platform for the drug. In addition to the full solid-state characterization of the composites and the *in vitro* study of the release of both heparin and biochanin A, the protein adhesion and hemocompatibility were evaluated. This study revealed that the copolymer composite was non-thrombogenic, which is a positive starting point in the use of inorganic ingredients for the development of VS.

In view of the number of studies using SMP for the manufacturing of VS, it is possible to state that “smart materials” have arrived to stay^[134,135]. The usefulness of smart materials in the development of cardiovascular devices (not only VS) has been demonstrated by the number of already commercialized VS made of nitinol (SMA), i.e., VascuFlex® or S.M.A.R.T™ Flex, among others. Others like ferromagnetic SMA are also drawing attention^[135] and can also be 3D-printed. Even if much remains to be done, especially when it comes to 3D-printed VS, it is clear that SMP offer attractive features, from their self-expanding property to the biocompatibility, biodegradability and drug-eluting features, not to mention the possibility of being compatible with different 3DP techniques. The range of future possibilities is even greater if we consider SMP functionalization, surface modifications or their use as part of nanocomposites^[106,136].

Another important factor, which is sometimes overlooked, is the resolution of the final construct and how the selection of the 3DP technique influences it. It is well-known that the resolution depends on a wide variety of factors, not only on the 3DP technique itself. For instance, different 3D printers using the same technique can have strong differences in the final resolution depending on their particular features (e.g., the light source of DLP or SLA 3D printers^[137]), not to mention the different resolutions

that can be obtained by just changing the feedstock (e.g., some materials are more prone to “shrinking” than others after the printing process). In fact, the major part of the scientific efforts is focused on the manufacturing of BRS, which are made of polymers. Depending on the type of polymer, 3DP techniques such as FDM, MEX, DLP, SLA, PBF, and BJT can be used. Within this group, BJT and PBF can be highlighted in terms of resolution. On the contrary, FDM and MEX are the most frequently used and at the same time, the ones with lower resolution^[137-140].

Depending on the final use of the 3D construct and the required features, the selection of materials and/or 3DP technique can be restrictive factors, leaving limited room for resolution improvement. Although in some cases, the printing resolution may not be decisive for the performance of the printed structure (i.e., in dental prosthesis^[141]), we hypothesize that this factor could cause irregularities in VS that ultimately give rise to blood turbulences, let alone the necessity to accomplish manufacturing reproducibility and quality control. Post-treatment of the 3D-printed structures have demonstrated to be a valuable option to improve the final resolution of the VS^[137]. Computational studies could also be of use in predicting or quantifying the importance of structural changes and irregularities for the performance of the VS but they would not solve the root problem. The implementation of machine learning to 3DP could shed some light in this regard, since it will be useful not only for the design of the VS, but also in the optimization of printing parameters and *in situ* printing monitoring^[142-144].

8. Conclusions and challenges

Medical devices such as VS have revolutionized the treatment of cardiovascular diseases to the point that nowadays their implantation has become a routine, easily approachable surgical intervention for the treatment of stenosed vessels, especially in CAD. Throughout the years, stent technology has greatly evolved, from conventional, permanent, metallic vascular stents to the most outstanding designs such as bioresorbable, drug-eluting medical devices. In view of the wide variety of VS currently available in the market and the intelligent approaches for their production, vascular stenting is considered a mature, consolidated medical procedure. Nevertheless, a more efficient approach is required to address several medical and scientific challenges; most of them are related to the long-term effects jeopardizing stent patency, such as in-stent restenosis and thrombosis, especially PAD. Although bioresorbable and drug-eluting stents seemed to shed some light on this matter, it is still a challenge to optimize the mechanical properties of the stent and to have a total control over the stent degradation and drug release rate.

In this regard, 3DP enables the production of patient-specific medical devices, not only in terms of dimensions and shape, but also in mechanical properties. Thanks to the wide variety of techniques and materials, 3DP can be used not only to create the final medical device but also in combination with other traditional manufacturing methods to upgrade the final device: for instance, it is possible to create patient-specific sacrificial molds, controlled stent coating for drug control release, etc. 3DP is also a versatile technique that gives room for the easy change and production of different geometries and shapes that could also be of great importance to control or adjust the mechanical performance, degradation, and/or drug release rate of a VS. These features can also be adapted to the requirements and needs of each particular patient thanks to this manufacturing method. Nonetheless, there are limitations and flaws (e.g., limited resolution and subsequent lack of manufacturing reproducibility) that must be overcome for 3DP to become a realistic VS manufacturing option. Shape-memory polymers, though promising and easy to print, lack in mechanical performance. Moreover, the shapes of VS are rather intricate and difficult to achieve with 3DP techniques such as DED or MEX due to overhanging parts. The use of rotatory mandrels could solve this problem but the degree of customization could be limited. On the other side, SMA is an option for the manufacturing of VS, but their integration with 3DP is posing several difficulties: shape memory effect is not good, and printing parameters are difficult to optimize. The present review is concluded with a few major points:

- (i) Despite the different possibilities and stent type reviewed, the most used VS nowadays are metal-based, mainly because of their unbeatable mechanical properties. On the other hand, the 3DP of these VS is one of the most challenging techniques, as demonstrated by the absence of studies.
- (ii) The achievement of stents with optimal mechanical properties is a big challenge (even for the traditional manufacturing processes), since a proper compromise between axial flexibility and radial rigidity is crucial for a proper stent patency.
- (iii) Computational studies and machine learning are greatly useful for the rational design of VS, helping to accelerate the innovation of new structures and geometrical designs as well as to minimize some 3DP limitations such as in resolution.
- (iv) 3DP limitations can be minimized by strategically implementing it at different points or by combining it with other manufacturing techniques.

As for the type of materials, smart materials, such as SMA and shape-memory polymers, are potential candidates for use in future 3DP manufacturing of medical devices.

The incorporation of new materials could significantly improve the biocompatibility of the final medical device with respect to the most common devices available in the market.

Abbreviations

3DP	3D printing
BMS	Bare Metal Stent
BRS	Bioresorbable
CAD	Coronary Artery Disease
CDs	Cyclodextrins
CIP	Carbonyl iron powder
CNT	Carbon Nanotube
CVD	Chemical Vapor Deposition
DED	Directed Energy Deposition
DES	Drug eluting stent
DLP	Digital Light Processing
EC	Endothelial cells
FDM	Fused Deposition Modeling
GO	Graphene oxide
GR	Graphene
LDH	Layered Double Hydroxides (hydrotalcite-like clay minerals)
MDDS	Modified Drug Delivery System
mPDC	Metacrylated poly(1,12-dodecamethylene citrate)
MJT	Material Jetting
MWCNT	Multi-walled carbon nanotubes
PAD	Peripheral Artery Disease
PBF	Powder Bed Fusion
PCL	Polycaprolactone
PCLA	Poly(L-lactide-co- ϵ -caprolactone)
PDA	Polydopamine
PEDOT:PSS	Poli(3,4-etilendioxitiofeno)-poli(estireno sulfonato)
PEI	Polyethyleneimine
PGD	Poly(glycerol dodecanoate)
PGDA	Poly(glycerol dodecanoate acrylate)
PLA	Poly(lactic acid)
PLGA	Poly(lactic-co-glycolic acid)

PLLA	Poly (L-lactic acid)
PTA	Percutaneous Transluminal Angioplasty
PTCA	Percutaneous Transluminal Coronary Angioplasty
PU	Polyurethane
PVA	Polyvinyl alcohol
RPSC-CF	Rapid Prototyping Sacrificial Core-coating Forming
SE	Self-expanding or self-expandable
SLA	Stereolithography
PBF	Powder Bed Fusion (selective laser melting)
SMA	Shape Memory Alloy
SMC	Smooth muscle cells
SNAP	S-nitrosation of N-acetyl-d-penicillamine
SS	Stainless-steel
SWCNT	Single-walled carbon nanotubes
THF	Tetrahydrofuran
TPC	Thermoplastic copolyester elastomer
VEGF	Vascular endothelial growth factor
VPP	Vat Photopolymerization
VS	Vascular stent
β CD	β -cyclodextrin

Acknowledgments

None.

Funding

This work was funded by the Basque Country Government/Eusko Jaurlaritz (Department of Education, University and Research, Consolidated Groups IT448-22). Sandra Ruiz-Alonso and Fouad Al-Hakim thank the Basque Country Government for the granted fellowships PRE_2021_2_0153 and PRE_2021_2_0181, respectively. Denis Scaini gratefully acknowledges support from IKERBASQUE, the Basque Foundation of Science.

Conflict of interest

The authors declare no conflicts of interests.

Author contributions

Conceptualization: Fernando Lopez-Zarraga, Denis Scaini, Jose Luis Pedraz.

Funding acquisition: Laura Saenz-del-Burgo, Jose Luis Pedraz.

Formal analysis: Fatima Garcia-Villen, Irene Diez-Aldama, Fouad Al-Hakim.

Visualization: Fatima Garcia-Villen.

Supervision: Fernando Lopez-Zarraga, Cesar Viseras, Denis Scaini.

Writing – original draft: Fatima Garcia-Villen, Sandra Ruiz-Alonso, Irene Diez-Aldama.

Writing – review & editing: Fernando Lopez-Zarraga, Laura Saenz-del-Burgo, Denis Scaini, Cesar Viseras, Jose Luis Pedraz.

Ethics approval and consent to participate

Not applicable.

Consent for publication

Not applicable.

Availability of data

Not applicable.

References

- Herrington W, Lacey B, Sherliker P, *et al.*, 2016, Epidemiology of atherosclerosis and the potential to reduce the global burden of atherothrombotic disease. *Circ Res*, 118(4):535–546.
<https://doi.org/10.1161/CIRCRESAHA.115.307611>
- Song P, Fang Z, Wang H, *et al.*, 2020, Global and regional prevalence, burden, and risk factors for carotid atherosclerosis: A systematic review, meta-analysis, and modelling study. *Lancet Glob Health*, 8(5):e721–e729.
[https://doi.org/10.1016/S2214-109X\(20\)30117-0/ATTACHMENT/B6277D32-2818-4A94-B438-584B317D09A4/MMC1.PDF](https://doi.org/10.1016/S2214-109X(20)30117-0/ATTACHMENT/B6277D32-2818-4A94-B438-584B317D09A4/MMC1.PDF)
- WHO, 2020, *World Health Statistics 2020: Monitoring Health for the SDGs, Sustainable Development Goals*. World Health Organization 2020 (WHO).
- Poredoš P, Jug B, 2007, The prevalence of peripheral arterial disease in high risk subjects and coronary or cerebrovascular patients. *Angiology*, 58(3):309–315.
<https://doi.org/10.1177/0003319707302494>
- Bauersachs R, Zeymer U, Brière JB, *et al.*, 2019, Burden of coronary artery disease and peripheral artery disease: A literature review. *Cardiovasc Ther*. 2019(8295054), 1–9.
<https://doi.org/10.1155/2019/8295054>
- Virani SS, Alonso A, Aparicio HJ, *et al.*, 2021, Heart disease and stroke statistics—2021 update. *Circulation*, 143:E254–E743.
<https://doi.org/10.1161/CIR.0000000000000950>
- Juchniewicz H, Lubkowska A, 2020, Oxygen-ozone (O₂-O₃) therapy in peripheral arterial disease (PAD): A review study. *Ther Clin Risk Manag*, 16:579.
<https://doi.org/10.2147/TCRM.S255247>
- Ouriel K, Caves KM, Chaikof EL, *et al.*, 2006, The evolving impact of microfabrication and nanotechnology on stent design. *J Vasc Surg*, 44:1363–1368.
<https://doi.org/10.1016/j.jvs.2006.08.046>
- IMARC, 2022, Vascular stents market: Global industry trends, share, size, growth, opportunity and forecast 2022-2027. Accessed: April 09, 2022. [Online]. Available.
<https://www.imarcgroup.com/vascular-stents-market>
- Grüntzig A, 1978, Transluminal dilatation of coronary-artery stenosis. *Lancet (London, England)*, 1(8058):263.
[https://doi.org/10.1016/S0140-6736\(78\)90500-7](https://doi.org/10.1016/S0140-6736(78)90500-7)
- Lobato EB, 2019, Care of the patient with coronary stents undergoing noncardiac surgery, in *Essentials of Cardiac Anesthesia for Noncardiac Surgery: A Companion to Kaplan's Cardiac Anesthesia*, J. A. Kaplan, Ed. China, Elsevier, 33–69.
- Gao G, Yi H-G, Jiang W, *et al.*, 2022, A review on manufacturing and post-processing technology of vascular stents. *Micromachines*, 13(1):1–16.
<https://doi.org/10.3390/MI13010140>
- Uhlemann M, Möbius-Winkler S, Adam J, *et al.*, 2016, The Leipzig prospective drug-eluting balloon-registry – outcome of 484 consecutive patients treated for coronary in-stent restenosis and de novo lesions using paclitaxel-coated balloons. *Circ J*, 80(2):CJ-14-1352.
<https://doi.org/10.1253/CIRCJ.CJ-14-1352>
- Lee SJ, Jo HH, Lim KS, *et al.*, 2019, Heparin coating on 3D printed poly (L-lactic acid) biodegradable cardiovascular stent via mild surface modification approach for coronary artery implantation. *Chem Eng J*, 378(122116):1–15.
<https://doi.org/10.1016/J.CEJ.2019.122116>
- Beshchasna N, Saqib M, Kraskiewicz H, *et al.*, 2020, Recent advances in manufacturing innovative stents. *Pharmaceutics*, 12(349):1–36.
- Fontaine AB, Koelling K, Clay J, *et al.*, 1994, Decreased platelet adherence of polymer-coated tantalum stents. *J Vasc Interv Radiol*, 5(4):567–572.
[https://doi.org/10.1016/S1051-0443\(94\)71555-4](https://doi.org/10.1016/S1051-0443(94)71555-4)
- Borhani S, Hassanajili S, Tafti SHA, *et al.*, 2018, Cardiovascular stents: Overview, evolution, and next generation. *Prog Biomater* 2018 73, 7(3):175–205.
<https://doi.org/10.1007/S40204-018-0097-Y>

18. Ooi OC, Mullany CJ, Rihal CS, 2007, Revascularization options for ischemic heart disease: Coronary artery bypass grafting and percutaneous coronary intervention, in *Cardiovascular Therapeutics: A Companion to Braunwald's Heart Disease*, 3rd ed., E. M. Antman and M. S. Sabatine, Eds. W.B. Saunders, 157–177.
19. Scoutaris N, Chai F, Maurel B, *et al.*, 2015, Development and biological evaluation of inkjet printed drug coatings on intravascular stent. *Mol Pharm*, 13(1):125–133.
<https://doi.org/10.1021/ACS.MOLPHARMACEUT.5B00570>
20. Krankenberg H, *et al.*, 2017, Self-expanding versus balloon-expandable stents for iliac artery occlusive disease: The randomized ICE trial. *JACC Cardiovasc Interv*, 10(16):1694–1704.
<https://doi.org/10.1016/J.JCIN.2017.05.015>
21. Fornell D, 2019, Trends in coronary, carotid and peripheral stents | DAIC. *Diagn Interv Cardiol*.
<https://www.dicardiology.com/article/trends-coronary-carotid-and-peripheral-stents> (Accessed April 02, 2022)
22. van Haelst STW, Peeters Weem SMO, Moll FL, *et al.*, 2016, Current status and future perspectives of bioresorbable stents in peripheral arterial disease. *J Vasc Surg*, 64(4): 1151–1159.e1.
<https://doi.org/10.1016/J.JVS.2016.05.044>
23. Medical Advisory Secretariat, 2010, Stenting for peripheral artery disease of the lower extremities: An evidence-based analysis. *Ont Health Technol. Assess Ser*, 10(18):1–88. Accessed: April 02, 2022 [Online]. Available.
<https://pubmed.ncbi.nlm.nih.gov/23074395/>
24. Klabunde RE, 2017, Coronary anatomy and blood flow. *Cardiovasc Physiol Concepts*.
<https://www.cvphysiology.com/Blood Flow/BF001> (Accessed April 02, 2022).
25. Klabunde RE, 2010, Autoregulation of organ blood flow. *Cardiovas Physiol Concepts*.
<https://www.cvphysiology.com/Blood Flow/BF004> (Accessed April 02, 2022).
26. Mani G, Feldman MD, Patel D, *et al.*, 2007, Coronary stents: A materials perspective. *Biomaterials*, 28(9):1689–1710.
<https://doi.org/10.1016/J.BIOMATERIALS.2006.11.042>
27. Lachowitz M, 2008, Assessing radial tests for endovascular implants. *Med Device Diagn Ind*.
<https://www.mddionline.com/news/assessing-radial-tests-endovascular-implants> (Accessed February 02, 2022).
28. Stoeckel D, Bonsignore C, Duda S, 2002, A survey of stent designs. *Minim Invasive Ther Allied Technol*, 11(4):137–147. Accessed: February 02, 2022 [Online]. Available.
<https://sci-hub.ru/https://www.tandfonline.com/doi/abs/10.1080/136457002760273340>
29. Abhyankar AD, Thakkar AS, 2012, In vivo assessment of stent recoil of biodegradable polymer-coated cobalt-chromium sirolimus-eluting coronary stent system. *Indian Heart J*, 64(6):546.
<https://doi.org/10.1016/J.IHJ.2012.07.005>
30. Lee MS, Banka G, 2016, In-stent restenosis. *Interv Cardiol Clin*, 5(2):211–220.
<https://doi.org/10.1016/J.ICCL.2015.12.006>
31. Modi K, Soos MP, Mahajan K, 2021, Stent thrombosis. *StatPearls* 1–15. Accessed: February 03, 2022 [Online]. Available.
<https://www.ncbi.nlm.nih.gov/books/NBK441908/>
32. Reejhsinghani R, Lotfi AS, 2015, Prevention of stent thrombosis: Challenges and solutions. *Vasc Health Risk Manag*, 2015(11):93–106.
<https://doi.org/10.2147/VHRM.S43357>
33. Kolandaivelu K, Swaminathan R, Gibson WJ, *et al.*, 2011, Stent thrombogenicity early in high-risk interventional settings is driven by stent design and deployment and protected by polymer-drug coatings. *Circulation*, 123(13):1400–1409.
<https://doi.org/10.1161/CIRCULATIONAHA.110.003210>
34. Hotta E, Hara H, Kamiya T, *et al.*, 2018, Non-thermal atmospheric pressure plasma-induced IL-8 expression is regulated via intracellular K⁺ loss and subsequent ERK activation in human keratinocyte HaCaT cells. *Arch Biochem Biophys*, 644:64–71.
<https://doi.org/10.1016/j.abb.2018.03.005>
35. Cvrček L, Horáková M, 2019, Plasma modified polymeric materials for implant applications, in *Non-Thermal Plasma Technology for Polymeric Materials. Applications in Composites, Nanostructured Materials and Biomedical Fields.*, S. Thomas, M. Mozetič, U. Cvelbar, *et al.*, Eds. Elsevier, 367–407.
36. Guo R, He Y, Li H, *et al.*, 2020, Development of 3D-printed sulfated chitosan modified bioresorbable stents for coronary artery disease. *Front Bioeng Biotechnol*, 8(462):1–12.
<https://doi.org/10.3389/fbioe.2020.00462>
37. Demir AG, Previtali B, 2017, Additive manufacturing of cardiovascular CoCr stents by selective laser melting. *Mater Des*, 119:338–350.
<https://doi.org/10.1016/J.MATDES.2017.01.091>
38. Zou Q, Xue W, Lin J, *et al.*, 2016, Mechanical characteristics of novel polyester/NiTi wires braided composite stent for the medical application. *Results Phys*, 6:440–446.
<https://doi.org/10.1016/J.RINP.2016.07.007>
39. Ahlhelm F, Kaufmann R, Ahlhelm D, *et al.*, 2009, Carotid artery stenting using a novel self-expanding braided nickel-

- titanium stent: Feasibility and safety porcine trial. *Cardiovasc Interv Radiol*, 32(5):1019–1027.
<https://doi.org/10.1007/S00270-009-9572-0>
40. Ueng KC, Wen SP, Lou CW, *et al.*, 2016, Stainless steel/nitinol braid coronary stents: Braiding structure stability and cut section treatment evaluation. *J Ind Text*, 45(5):965–977.
<https://doi.org/10.1177/1528083714550054>
41. Marti P, Lampus F, Benevento D, *et al.*, 2019, Trends in use of 3D printing in vascular surgery: A survey. *Int Angiol*, 38(5):418–424.
<https://doi.org/10.23736/S0392-9590.19.04148-8>
42. Memon S, Friend E, Samuel SP, *et al.*, 2021, 3D printing of carotid artery and aortic arch anatomy: Implications for preprocedural planning and carotid stenting. *J Invasive Cardiol*, 33(9):E723–E729. Accessed: December 30, 2021 [Online]. Available.
<https://pubmed.ncbi.nlm.nih.gov/34473073/>
43. Valverde I, Gomez G, Coserria JF, *et al.*, 2015, 3D printed models for planning endovascular stenting in transverse aortic arch hypoplasia. *Catheter Cardiovasc Interv*, 85(6):1006–1012.
<https://doi.org/10.1002/CCD.25810>
44. Sun Z, Jansen S, 2019, Personalized 3D printed coronary models in coronary stenting. *Quant Imaging Med Surg*, 9(8):1356–1367.
<https://doi.org/10.21037/QIMS.2019.06.21>
45. Bortman J, Mahmood F, Schermerhorn M, *et al.*, 2019, Use of 3-dimensional printing to create patient-specific abdominal aortic aneurysm models for preoperative planning. *J Cardiothorac Vasc Anesth*, 33(5):1442–1446.
<https://doi.org/10.1053/J.JVCA.2018.08.011>
46. Barón V, Guevara R, 2019, Three-dimensional printing-guided fenestrated endovascular aortic aneurysm repair using open source software and physician-modified devices. *J Vasc Surg Cases Innov Tech*, 5(4):566–571.
<https://doi.org/10.1016/J.JVSCIT.2019.08.006>
47. Young L, Harb SC, Puri R, *et al.*, 2020, Percutaneous coronary intervention of an anomalous coronary chronic total occlusion: The added value of three-dimensional printing. *Catheter Cardiovasc Interv*, 96(2):330–335.
<https://doi.org/10.1002/CCD.28625>
48. Walker JL, Santoro M, 2017, Processing and production of bioresorbable polymer scaffolds for tissue engineering, in *Bioresorbable Polymers for Biomedical Applications: From Fundamentals to Translational Medicine*, G. Perale and J. Hilborn, Eds. Woodhead Publishing, 181–203.
49. Singh R, Singh S, Hashmi MSJ, 2016, Implant materials and their processing technologies, in *Materials Science and Materials Engineering*, Elsevier.
50. Mohapatra S, Kar RK, Biswal PK, *et al.*, 2022, Approaches of 3D printing in current drug delivery. *Sensors Int*, 3(100146): 1–10.
<https://doi.org/10.1016/J.SINTL.2021.100146>
51. Schwab A, Levato R, D'Este M, *et al.*, 2020, Printability and shape fidelity of bioinks in 3D bioprinting. *Chem Rev*, 120(19):11028–11055.
<https://doi.org/10.1021/acs.chemrev.0c00084>
52. Garcia-Villen F, Ruiz-Alonso S, Lafuente-Merchan M, *et al.*, 2021, Clay minerals as bioink ingredients for 3D printing and 3D bioprinting: Application in tissue engineering and regenerative medicine. *Pharmaceutics*, 13(1806):1–46. [Online]. Available.
<https://pubmed.ncbi.nlm.nih.gov/34834221/>
53. Manita PG, Garcia-Orue I, Santos-Vizcaino E, *et al.*, 2021, 3D bioprinting of functional skin substitutes: From current achievements to future goals. *Pharmaceutics*, 14(362): 1–25. [Online]. Available.
<https://www.mdpi.com/1424-8247/14/4/362>
54. Jamee R, Araf Y, Bin Naser I, *et al.*, 2021, The promising rise of bioprinting in revolutionizing medical science: Advances and possibilities. *Regen Ther*, 18:133–145.
<https://doi.org/10.1016/J.RETH.2021.05.006>
55. Begum S, Karim ANM, Ansari MNM, *et al.*, 2020, Nanomaterials, in *Encyclopedia of Renewable and Sustainable Materials*, vol. 1, S. Hashmi and I. A. Choudhury, Eds. Elsevier, 515–539.
56. Song X, Zhai W, Huang R, *et al.*, 2022, Metal-based 3D-printed micro parts & structures, in *Encyclopedia of Materials: Metals and Alloys*, vol. 4, F. G. Caballero, Ed. Elsevier, 448–461.
57. Zhu C, Liu T, Qian F, *et al.*, 2017, 3D printed functional nanomaterials for electrochemical energy storage. *Nano Today*, 15:107–120.
<https://doi.org/10.1016/J.NANTOD.2017.06.007>
58. Xu C, Bouchemit A, L'Espérance G, *et al.*, 2017, Solvent-cast based metal 3D printing and secondary metallic infiltration. *J Mater Chem C*, 5(40):10448–10455.
<https://doi.org/10.1039/C7TC02884A>
59. Guerra AJ, Cano P, Rabionet M, *et al.*, 2018, 3D-printed PCL/PLA composite stents: Towards a new solution to cardiovascular problems. *Materials (Basel, Switzerland)*, 11(9): 1–13.
<https://doi.org/10.3390/MA11091679>
60. Guerra AJ, Ciurana J, 2018, 3D-printed bioabsorbable polycaprolactone stent: The effect of process parameters on its physical features. *Mater Design*, 137:430–437.
<https://doi.org/10.1016/J.MATDES.2017.10.045>

61. Wu Z, Zhao J, Wu W, *et al.*, 2017, A novel 3D additive manufacturing machine to biodegradable stents. *Proc Manuf*, 13:718–723.
<https://doi.org/10.1016/J.PROMFG.2017.09.118>
62. Wu Z, *et al.*, 2018, Radial compressive property and the proof-of-concept study for realizing self-expansion of 3D printing polylactic acid vascular stents with negative Poisson's ratio structure. *Materials (Basel)*, 11(8):1357.
<https://doi.org/10.3390/MA11081357>
63. Jia H, Gu SY, Chang K, 2018, 3D printed self-expandable vascular stents from biodegradable shape memory polymer. *Adv Polym Technol*, 37(8):3222–3228.
<https://doi.org/10.1002/ADV.22091>
64. Zhang C, Cai D, Liao P, *et al.*, 2021, 4D printing of shape-memory polymeric scaffolds for adaptive biomedical implantation. *Acta Biomater*, 122:101–110.
<https://doi.org/10.1016/J.ACTBIO.2020.12.042>
65. Kim D, Kim T, Lee YG, 2019, 4D printed bifurcated stents with kirigami-inspired structures. *J Vis Exp*, 149(e59746):1–9.
<https://doi.org/10.3791/59746>
66. Kim T, Lee Y-G, 2018, Shape transformable bifurcated stents. *Sci Rep*, 8(13911):1–9.
<https://doi.org/10.1038/s41598-018-32129-3>
67. Zhang Y, Zhao J, Yang G, *et al.*, 2019, Mechanical properties and degradation of drug eluted bioresorbable vascular scaffolds prepared by three-dimensional printing technology. *J Biomater Sci Polym Ed*, 30(7):547–560.
<https://doi.org/10.1080/09205063.2019.1586303>
68. Lei Y, Chen X, Li Z, *et al.*, 2020, A new process for customized patient-specific aortic stent graft using 3D printing technique. *Med Eng Phys*, 77:80–87.
<https://doi.org/10.1016/j.medengphy.2019.12.002>
69. Park SA, Lee SJ, Lim KS, *et al.*, 2015, In vivo evaluation and characterization of a bio-absorbable drug-coated stent fabricated using a 3D-printing system. *Mater Lett*, 141: 355–358.
<https://doi.org/10.1016/J.MATLET.2014.11.119>
70. Misra SK, Ostadhossein F, Babu R, *et al.*, 2017, 3D-printed multidrug-eluting stent from graphene-nanoplatelet-doped biodegradable polymer composite. *Adv Healthc Mater*, 6(1700008):1–14.
<https://doi.org/10.1002/ADHM.201700008>
71. Zhou Y, Zhou D, Cao P, *et al.*, 2021, 4D printing of shape memory vascular stent based on β CD-g-polycaprolactone. *Macromol Rapid Commun*, 42(14):2100176.
<https://doi.org/10.1002/MARC.202100176>
72. Singh J, Kaur T, Singh N, *et al.*, 2020, Biological and mechanical characterization of biodegradable carbonyl iron powder/polycaprolactone composite material fabricated using three-dimensional printing for cardiovascular stent application. *Proc Inst Mech Eng H*, 234(9):975–987.
<https://doi.org/10.1177/0954411920936055>
73. Van Lith R, Baker E, Ware H, *et al.*, 2016, 3D-printing strong high-resolution antioxidant bioresorbable vascular stents. *Adv Mater Technol*, 1(9): 1–7.
<https://doi.org/10.1002/ADMT.201600138>
74. Ware HOT, Farsheed AC, Akar B, *et al.*, 2018, High-speed on-demand 3D printed bioresorbable vascular scaffolds. *Mater Today Chem*, 7:25–34.
<https://doi.org/10.1016/J.MTCHEM.2017.10.002>
75. de Oliveira MF, da Silva LCE, de Oliveira MG, 2021, 3D printed bioresorbable nitric oxide-releasing vascular stents. *Bioprinting*, 22(e00137): 1–10.
<https://doi.org/10.1016/J.BPRINT.2021.E00137>
76. Yang J, Webb AR, Pickerill SJ, *et al.*, 2006, Synthesis and evaluation of poly(diols citrate) biodegradable elastomers. *Biomaterials*, 27(9):1889–1898.
<https://doi.org/10.1016/J.BIOMATERIALS.2005.05.106>
77. Ismael A, Papoutsi E, Miserlis D, *et al.*, 2020, The nitric oxide system in peripheral artery disease: Connection with oxidative stress and biopterins. *Antioxidants*, 9(7):1–16.
<https://doi.org/10.3390/ANTIOX9070590>
78. Flege C, Vogt F, Höges S, *et al.*, 2013, Development and characterization of a coronary polylactic acid stent prototype generated by selective laser melting. *J Mater Sci Mater Med*, 24(1):241–255.
<https://doi.org/10.1007/S10856-012-4779-Z>
79. Elliott MR, Kim D, Molony DS, *et al.*, 2019, Establishment of an automated algorithm utilizing optical coherence tomography and micro-computed tomography imaging to reconstruct the 3-D deformed stent geometry. *IEEE Trans Med Imaging*, 38(3):710–720.
<https://doi.org/10.1109/TMI.2018.2870714>
80. Wiesent L, Spear A, Nonn A, 2022, Computational analysis of the effects of geometric irregularities on the interaction of an additively manufactured 316L stainless steel stent and a coronary artery. *J Mech Behav Biomed Mater*, 125:1–12.
<https://doi.org/10.1016/J.JMBBM.2021.104878>
81. Chiastra C, Mazzi V, Lodi Rizzini M, *et al.*, 2022, Coronary artery stenting affects wall shear stress topological skeleton. *J Biomech Eng*. 144(6):061002, 1–11.
<https://doi.org/10.1115/1.4053503>
82. Pan C, Han Y, Lu J, 2021, Structural design of vascular stents: A review. *Micromachines*, 12(7):770.
<https://doi.org/10.3390/MI12070770>

83. Habib A, Finn AV, 2015, Endothelialization of drug eluting stents and its impact on dual anti-platelet therapy duration. *Pharmacol Res*, 93:22–27.
<https://doi.org/10.1016/J.PHRS.2014.12.003>
84. Nguyen DT, Smith AF, Jiménez JM, 2021, Stent strut streamlining and thickness reduction promote endothelialization. *J R Soc Interface*, 18(181):1–14.
<https://doi.org/10.1098/RSIF.2021.0023>
85. Cabrera MS, Sanders B, Goor OLG, *et al.*, 2017, Computationally designed 3D printed self-expandable polymer stents with biodegradation capacity for minimally invasive heart valve implantation: a proof-of-concept study. *3D Print Addit Manuf*, 4(1):19–29.
<https://doi.org/10.1089/3DP.2016.0052/ASSET/IMAGES/LARGE/FIGURE8.JPEG>
86. Vellayappan MV, Balaji A, Subramanian AP, *et al.*, 2015, Multifaceted prospects of nanocomposites for cardiovascular grafts and stents. *Int J Nanomed*, 10:2785–2803.
<https://doi.org/10.2147/IJN.S80121>
87. Chou TC, Fu E, Wu CJ, *et al.*, 2003, Chitosan enhances platelet adhesion and aggregation. *Biochem Biophys Res Commun*, 302(3):480–483.
[https://doi.org/10.1016/S0006-291X\(03\)00173-6](https://doi.org/10.1016/S0006-291X(03)00173-6)
88. Wickham AM, Islam MM, Mondal D, *et al.*, 2014, Polycaprolactone–thiophene-conjugated carbon nanotube meshes as scaffolds for cardiac progenitor cells. *J Biomed Mater Res Part B Appl Biomater*, 102(7):1553–1561.
<https://doi.org/10.1002/JBM.B.33136>
89. Stout DA, Yoo J, Santiago-Miranda AN, *et al.*, 2012, Mechanisms of greater cardiomyocyte functions on conductive nanoengineered composites for cardiovascular application. *Int J Nanomed*, 7:5653–5669.
<https://doi.org/10.2147/IJN.S34574>
90. Mattioli-Belmonte M, Vozzi G, Whulanza Y, *et al.*, 2012, Tuning polycaprolactone–carbon nanotube composites for bone tissue engineering scaffolds. *Mater Sci Eng C*, 32(2):152–159.
<https://doi.org/10.1016/J.MSEC.2011.10.010>
91. Chakoli AN, Wan J, Feng JT, *et al.*, 2009, Functionalization of multiwalled carbon nanotubes for reinforcing of poly(l-lactide-co-ε-caprolactone) biodegradable copolymers. *Appl Surf Sci*, 256(1):170–177.
<https://doi.org/10.1016/J.APSUSC.2009.07.103>
92. Lee HH, Shin US, Jin GZ, *et al.*, 2011, Highly homogeneous carbon nanotube-polycaprolactone composites with various and controllable concentrations of ionically-modified-MWCNTs. *Bull Korean Chem Soc*, 32(1):157–161.
<https://doi.org/10.5012/BKCS.2011.32.1.157>
93. Arabi H, Mirzadeh H, Ahmadi SH, *et al.*, 2004, In vitro and in vivo hemocompatibility evaluation of graphite coated polyester vascular grafts. *Int J Artif Organs* 27(8):691–698.
<https://doi.org/10.1177/039139880402700807>
94. Podila R, Moore T, Alexis F, *et al.*, 2013, Graphene coatings for biomedical implants. *J Vis Exp*, 73(e50276):1–9.
<https://doi.org/10.3791/50276>
95. Gao F, Hu Y, Li G, *et al.*, 2020, Layer-by-layer deposition of bioactive layers on magnesium alloy stent materials to improve corrosion resistance and biocompatibility. *Bioact Mater*, 5(3):611–623.
<https://doi.org/10.1016/J.BIOACTMAT.2020.04.016>
96. Yang MC, Tsou HM, Hsiao YS, *et al.*, 2019, Electrochemical polymerization of PEDOT-graphene oxide-heparin composite coating for anti-fouling and anti-clotting of cardiovascular stents. *Polymers (Basel)*, 11(9):1–15.
<https://doi.org/10.3390/POLYM11091520>
97. Alshebly YS, Nafea M, Mohamed Ali MS, *et al.*, 2021, Review on recent advances in 4D printing of shape memory polymers. *Eur Polym J*, 159:110708.
<https://doi.org/10.1016/J.EURPOLYMJ.2021.110708>
98. Melocchi A, Uboldi M, Cerea M, *et al.*, 2021, Shape memory materials and 4D printing in pharmaceuticals. *Adv Drug Deliv Rev*, 173:216–237.
<https://doi.org/10.1016/J.ADDR.2021.03.013>
99. Xu J, Zhang Y, Feng YB, *et al.*, 2018, Electromagnetic and mechanical properties of carbonyl iron powder-filled methyl vinyl silicone rubber during thermal aging. *Polym Compos*, 39(8):2897–2903.
<https://doi.org/10.1002/PC.24286>
100. Waksman R, Pakala R, Baffour R, *et al.*, 2008, Short-term effects of biocorrosible iron stents in porcine coronary arteries. *J Interv Cardiol*, 21(1):15–20.
<https://doi.org/10.1111/J.1540-8183.2007.00319.X>
101. Peuster M, Hesse C, Schloo T, *et al.*, 2006, Long-term biocompatibility of a corrodible peripheral iron stent in the porcine descending aorta. *Biomaterials*, 27(28):4955–4962.
<https://doi.org/10.1016/J.BIOMATERIALS.2006.05.029>
102. Peuster M, Wohlsein P, Brüggemann M, *et al.*, 2001, A novel approach to temporary stenting: Degradable cardiovascular stents produced from corrodible metal-results 6-18 months after implantation into New Zealand white rabbits. *Heart*, 86(5):563–569.
<https://doi.org/10.1136/HEART.86.5.563>
103. Liu B, Zheng YF, 2011, Effects of alloying elements (Mn, Co, Al, W, Sn, B, C and S) on biodegradability and in vitro biocompatibility of pure iron. *Acta Biomater*, 7(3):1407–1420.
<https://doi.org/10.1016/J.ACTBIO.2010.11.001>

104. Khoo ZX, Liu Y, An J, *et al.*, 2018, A review of selective laser melted NiTi shape memory alloy. *Material*, 11:519.
<https://doi.org/10.3390/MA11040519>
105. Biffi CA, Fiocchi J, Valenza F, 2020, *et al.*, Selective laser melting of NiTi shape memory alloy: Processability, microstructure, and superelasticity. *Shape Mem Superelasticity*, 6(3):342–353.
<https://doi.org/10.1007/S40830-020-00298-8/FIGURES/11>
106. Safavi MS, Bordbar-Khiabani A, Khalil-allafi J, *et al.*, 2022, Additive manufacturing: An opportunity for the fabrication of near-net-shape NiTi implants. *J Manuf Mater Process*, 6(3):1–22.
<https://doi.org/10.3390/JMMP6030065>
107. Hassani FA, Peh WYX, Gammad GGL, *et al.*, 2017, A 3D printed implantable device for voiding the bladder using shape memory alloy (SMA) actuators. *Adv Sci*, 4(11):1–10.
<https://doi.org/10.1002/ADVS.201700143>
108. Tong A, Pham QL, Abatamarco P, *et al.*, 2021, Review of low-cost 3D bioprinters: State of the market and observed future trends. *SLAS Technol*, 26(4):333–366.
<https://doi.org/10.1177/24726303211020297>
109. Choonara YE, Du Toit LC, Kumar P, *et al.*, 2016, 3D-printing and the effect on medical costs: A new era? *Expert Rev Pharmacoecon Outcomes Res*, 16(1):23–32.
<https://doi.org/10.1586/14737167.2016.1138860>
110. van Tonder L, Labuschagné FJWJ, 2021, Systematic literature review of the effect of layered double hydroxides on the mechanical properties of rubber. *Polymer*, 13:3716.
<https://doi.org/10.3390/POLYM13213716>
111. Coppola B, Cappetti N, Di Maio L, *et al.*, 2017, Layered silicate reinforced polylactic acid filaments for 3D printing of polymer nanocomposites, 1–4.
<https://doi.org/10.1109/RTSI.2017.8065892>
112. Papageorgiou DG, Li Z, Liu M, *et al.*, 2020, Mechanisms of mechanical reinforcement by graphene and carbon nanotubes in polymer nanocomposites. *Nanoscale*, 12(4. Royal Society of Chemistry): 2228–2267.
<https://doi.org/10.1039/c9nr06952f>
113. Coleman JN, Khan U, Gun'ko YK, 2006, Mechanical reinforcement of polymers using carbon nanotubes. *Adv Mater*, 18(6):689–706.
<https://doi.org/10.1002/ADMA.200501851>
114. Kim H, Ryu KH, Baek D, *et al.*, 2020, 3D printing of polyethylene terephthalate glycol-sepiolite composites with nanoscale orientation. *ACS Appl Mater Interfaces*, 12(20):23453–23463.
<https://doi.org/10.1021/acsami.0c03830>
115. Zhou K, Dey M, Ayan B, *et al.*, 2021, Fabrication of PDMS microfluidic devices using nanoclay-reinforced Pluronic F-127 as a sacrificial ink. *Biomed Mater*, 16(4):45005.
<https://doi.org/10.1088/1748-605X/abe55e>
116. Gu Z, Rolfe BE, Xu ZP, *et al.*, 2012, Antibody-targeted drug delivery to injured arteries using layered double hydroxide nanoparticles. *Adv Healthc Mater*, 1(5):669–673.
<https://doi.org/10.1002/ADHM.201200069>
117. Gu Z, Rolfe B, Thomas A, *et al.*, 2013, Restenosis treatments using nanoparticle-based drug delivery systems. *Curr Pharm Des*, 19(35):6330–6339.
<https://doi.org/10.2174/1381612811319350009>
118. Gu Z, Rolfe BE, Xu ZP, *et al.*, 2010, Enhanced effects of low molecular weight heparin intercalated with layered double hydroxide nanoparticles on rat vascular smooth muscle cells. *Biomaterials*, 31(20):5455–5462.
<https://doi.org/10.1016/J.BIOMATERIALS.2010.03.050>
119. Ishihara S, Machino T, Deguchi K, *et al.*, 2021, Disposable nitric oxide generator based on a structurally deformed nitrite-type layered double hydroxide. *Inorg Chem*, 60(21):16008–16015.
<https://doi.org/10.1021/ACS.INORGCHEM.1C00456>
120. Russell SE, González Carballo JM, Orellana-Tavra C, *et al.*, 2017, A comparison of copper and acid site zeolites for the production of nitric oxide for biomedical applications. *Dalt Trans*, 46(12):3915–3920.
<https://doi.org/10.1039/C7DT00195A>
121. Doyle RA, Russell SE, Morris RE, 2019, Nitric oxide production from nitrite by a series of zeolites produced via the ADOR route. *Microporous Mesoporous Mater*, 280:367–371.
<https://doi.org/10.1016/J.MICROMESO.2019.02.019>
122. Jung SY, Kim HM, Hwang S, *et al.*, 2020, Physicochemical properties and hemocompatibility of layered double hydroxide-based anticancer drug methotrexate delivery system. *Pharm*, 12:1210.
<https://doi.org/10.3390/PHARMACEUTICS12121210>
123. Gu Z, Yan S, Cheong S, *et al.*, 2018, Layered double hydroxide nanoparticles: Impact on vascular cells, blood cells and the complement system. *J Colloid Interface Sci*, 512:404–410.
<https://doi.org/10.1016/J.JCIS.2017.10.069>
124. Vaiana CA, Leonard MK, Drummy LF, *et al.*, 2011, Epidermal growth factor: Layered silicate nanocomposites for tissue regeneration. *Biomacromolecules*, 12(9):3139–3146.
<https://doi.org/10.1021/bm200616v>
125. Wu K, Feng R, Jiao Y, *et al.*, 2017, Effect of halloysite nanotubes on the structure and function of important multiple blood components. *Mater Sci Eng C*, 75:72–78.
<https://doi.org/10.1016/J.MSEC.2017.02.022>

126. Devlin JJ, Kircher S, Kozen BG, *et al.*, 2011, Comparison of ChitoFlex®, CELOX™, and QuikClot® in control of hemorrhage. *J Emerg Med*, 41(3):237–245.
<https://doi.org/http://dx.doi.org/10.1016/j.jemermed.2009.02.017>
127. Ran Y, *et al.*, 2010, QuikClot combat gauze use for hemorrhage control in military trauma: January 2009 Israel Defense Force Experience in the Gaza Strip—A preliminary report of 14 cases. *Prehosp Disaster Med*, 25(6):584–588 [Online]. Available:
<http://journals.cambridge.org/action/displayAbstract?fromPage=online&aid=8257157&fileId=S1049023X00008797>
128. Choi SJ, Oh JM, Choy JH, 2008, Safety aspect of inorganic layered nanoparticles: Size-dependency in vitro and in vivo. *J Nanosci Nanotechnol*, 8(10):5297–5301.
<https://doi.org/10.1166/JNN.2008.1143>
129. Tahmasebi-Birgani Z, Solati-Hashjin M, Peirovi H, *et al.*, 2010, Layered double hydroxide: A new ceramid-based hemostatic agent?, in *Ceramic Transactions*, vol. 218, R. Narayan, M. Singh, and McKittrick, Eds. Wiley-American Ceramic Society, 53–57.
130. Mahesh V, Joseph AS, Mahesh V, *et al.*, 2021, Investigation on the mechanical properties of additively manufactured PETG composites reinforced with OMMT nanoclay and carbon fibers. *Polym Compos*, 42:2380–2395.
<https://doi.org/10.1002/pc.25985>
131. Coppola B, Cappetti N, Di Maio L, *et al.*, 2018, 3D printing of PLA/clay nanocomposites: Influence of printing temperature on printed samples properties. *Materials (Basel)*, 11(1947):1–17.
<https://doi.org/10.3390/ma11101947>
132. Paspali A, Bao Y, Gawne DT, *et al.*, 2018, The influence of nanostructure on the mechanical properties of 3D printed polylactide/nanoclay composites. *Compos Part B Eng*, 152:160–168.
<https://doi.org/10.1016/j.compositesb.2018.07.005>
133. Adepu S, Luo H, Ramakrishna S, 2021, Heparin-tagged PLA-PEG copolymer-encapsulated biochanin A-loaded (Mg/Al) LDH nanoparticles recommended for non-thrombogenic and anti-proliferative stent coating. *Int J Mol Sci*, 22(11):5433.
<https://doi.org/10.3390/IJMS22115433/S1>
134. Xiao R, Huang WM, Xiao R, *et al.*, 2020, Heating/solvent responsive shape-memory polymers for implant biomedical devices in minimally invasive surgery: Current status and challenge. *Macromol Biosci*, 20(8):2000108.
<https://doi.org/10.1002/MABI.202000108>
135. Bhatia M, Bhatia S, Siddhartha, 2022, Smart materials for cardiovascular devices. *Mater Today Proc*, 53:307–309.
<https://doi.org/10.1016/J.MATPR.2021.12.591>
136. Jiang JJ, Hu Y, Chen X, *et al.*, 2018, Development and application of shape memory intelligent composites. *Cailiao Gongcheng/J Mater Eng*, 46(8):1–13.
<https://doi.org/10.11868/J.ISSN.1001-4381.2018.000344>
137. Hua W, Shi W, Mitchell K, *et al.*, 2022, 3D printing of biodegradable polymer vascular stents: A review. *Chin J Mech Eng Addit Manuf Front*, 1(2):100020.
<https://doi.org/10.1016/J.CJMEAM.2022.100020>
138. Kluska E, Gruda P, Majca-Nowak N, 2018, The accuracy and the printing resolution comparison of different 3D printing technologies. *Trans Aerosp Res*, 2018(3):69–86.
<https://doi.org/10.2478/TAR-2018-0023>
139. Nulty A, 2022, A comparison of trueness and precision of 12 3D printers used in dentistry. *BDJ Open*, 8(1):1–9.
<https://doi.org/10.1038/s41405-022-00108-6>
140. Chae MP, Chung RD, Smith JA, *et al.*, 2021, The accuracy of clinical 3D printing in reconstructive surgery: Literature review and in vivo validation study. *Gland Surg*, 10(7): 2293.
<https://doi.org/10.21037/GS-21-264>
141. Ho Kim J, Pinhata-Baptista OH, Ayres AP, *et al.*, 2022, Accuracy comparison among 3D-printing technologies to produce dental models. *Appl Sci*, 12(8425):1–9.
142. Nguyen PD, Nguyen TQ, Tao QB, *et al.*, 2022, A data-driven machine learning approach for the 3D printing process optimisation. *Virtual Phys Prototyp* 17(4):768–786.
<https://doi.org/10.1080/17452759.2022.2068446>
143. Gong X, Zeng D, Groeneveld-Meijer W, *et al.*, 2022, Additive manufacturing: A machine learning model of process-structure-property linkages for machining behavior of Ti-6Al-4V. *Mater Sci Addit Manuf*, 1(1):6.
<https://doi.org/10.18063/MSAM.V1I1.6>
144. Sing SL, Kuo CN, Shih CT, *et al.*, 2021, Perspectives of using machine learning in laser powder bed fusion for metal additive manufacturing. *Virtual Phys Prototyp* 16(3):372–386.
<https://doi.org/10.1080/17452759.2021.1944229>
145. Smolderen KG, Wang K, De Pouvourville G, *et al.*, 2012, Two-year vascular hospitalisation rates and associated costs in patients at risk of atherothrombosis in France and Germany: Highest burden for peripheral arterial disease. *Eur J Vasc Endovasc Surg*, 43(2):198–207.
<https://doi.org/10.1016/J.EJVS.2011.09.016>